NASA CR-112288

TR-3720359

Viking '75 Project

BALLOON LAUNCHED VIKING DECELERATOR TEST PROGRAM SUMMARY REPORT

NAS1-9000

MARTIN MARIETTA

(NASA-CR-112288) BALLOON LAUNCHED VIKING DECELERATOR TEST PROGRAM Summary Report (Martin Marietta Corp.) 81 p HC $6.25 CSCL 22B

N74-14534

Unclas

G3/31 26165

ABSTRACT

Four BLDT flights were conducted during the summer of 1972 over the White Sands Missile Range. The purpose of these tests was to qualify the Viking parachute system behind the full-scale Viking Entry Vehicle over the maximum range of entry conditions anticipated in the Viking '75 soft landing on Mars. Test concerns centered on the ability of the minimum weight parachute system to operate without fabric damage in the wake of the blunt-body entry vehicle. This is the first known instance of parachute operation at supersonic speeds in the wake of such a large blunt body. The flight tests utilized the largest successful balloon-payload weight combination known to reach the earth's upper atmosphere where a varying number of rocket engines were employed to boost the test vehicle to speeds and dynamic pressures simulating the range of conditions on Mars.

This report presents a summary of the test series. Test conditions ranged from a Mach number of 2.0 to 0.5 and dynamic pressure from 11.7 to 4.4 psf. This range of conditions covers the uncertainty in entry conditions at Mars due to atmospheric and entry performance uncertainties. The report emphasizes parachute performance and simulated Mars entry vehicle motions as influenced by the parachute performance. Conclusions are presented regarding the ability of the parachute to perform within the operational parameters required for a successful soft Martian landing. A list of references which covers all reports in the qualification test program is included.

James L. Raper

TR-3720359

March 1973

DRL Line Item No. N3-T042

BALLOON LAUNCHED VIKING DECELERATOR TEST PROGRAM SUMMARY REPORT

Prepared by

R. D. Moog

F. C. Michel

Approved by

Robert J. Polutchko
Project Engineer
Viking Vehicle Engineering

PREPARED UNDER CONTRACT NAS1-9000 BY
MARTIN MARIETTA CORPORATION
DENVER DIVISION
P.O. Box 179
DENVER, COLORADO 80201

PRECEDING PAGE BLANK NOT FILMED

TABLE OF CONTENTS

		Page
	TABLE OF CONTENTS	ii
	LIST OF ILLUSTRATIONS	iii
	LIST OF TABLES	v
I.	INTRODUCTION	1
II.	VIKING DECELERATOR SYSTEM	3
III.	TEST SYSTEM DESCRIPTION	7
IV.	MARS QUALIFICATION	11
V.	PARACHUTE DEPLOYMENT CONDITIONS	20
VI.	MORTAR PERFORMANCE	23
VII.	PARACHUTE INFLATION CHARACTERISTICS	26
VIII.	OPENING LOAD AND PREDICTION METHODS	31
IX.	PARACHUTE AND VEHICLE STABILITY	41
X.	AEROSHELL SEPARATION	49
XI.	PARACHUTE STRUCTURAL QUALIFICATION	53
XII.	PARACHUTE RECOVERY SUMMARY	56
XIII.	PARACHUTE DRAG PERFORMANCE	58
XIV.	CONCLUSIONS	72
XV.	REFERENCES	74

LIST OF ILLUSTRATIONS

Figure	Title	Page
1	Viking Decelerator System	5
2	Ejected Weight Distribution	6
3	Typical Mission Sequence - Powered Flight	8
4	BLDT Supersonic Vehicle Configuration	9
5	BLDT Supersonic Vehicle Sectional View	10
6	Mars Envelope and Test Conditions	14
7	BLDT AV-1 Test Conditions	15
8	BLDT AV-2 Test Conditions	16
9	BLDT AV-3 Test Conditions	17
10	BLDT AV-4 Test Conditions	18
11	Parachute Drag Coefficient Envelope	19
12	Parachute Filling Time Data	28
13	Canopy Growth Parameter	29
14	Canopy Area Oscillations	30
15	Wind Tunnel Drag Data	35
16	Suspension Line Load/Elongation Data	36
17	Predicted Versus Actual Load	37
18	Parachute Opening Load, BLDT AV-1	38
19	Parachute Opening Load, AV-2 and AV-3	39
20	Parachute Opening Load, BLDT AV-4	40
21	Vehicle Attitude Rates, AV-4 Flight Data	44
22	Vehicle Attitude Rates, AV-4 Simulation	45
23	Attitude Rate Sensitivity to Load	46
24	Selected Views of Parachute During Terminal Descent	47
25	Aeroshell Separation Conditions	51
26	Aeroshell Separation Distance	52
27	Parachute Cloth Stress During Inflation	55
28	Parachute Drag Coefficient	61
29	Parachute Lift	62
30	Horizontal Velocity Components, AV-1	63
31	Horizontal Velocity Components, AV-2	64
32	Horizontal Velocity Components, AV-3	65
33	Horizontal Velocity Components, AV-4	66

LIST OF ILLUSTRATIONS (CONTINUED)

Figure	Title	Page
34	Relative Velocity Phase Plane, AV-1 and AV-2	67
35	Relative Velocity Phase Plane, AV-3 and AV-4	68
36	Lift Vector Direction	69
37	Zero Lift Terminal Dynamic Pressure	70
38	Comparison Between LADT and BLDT Drag	71

LIST OF TABLES

Table	Title	Page
1	Parachute Geometric Properties	4
2	BLDT Parachute Deployment Conditions	21
3	BLDT Mortar Performance	25
4	Parachute Inflation Characteristics	26
5	BLDT Peak Load Conditions	33
6	Physical Property Data	42
7	BLDT Aeroshell Separation Conditions	50
8	Comparative Subsonic Test Data and Stress Predictions	54

I. INTRODUCTION

The purpose of this report is to summarize the results of qualification flight tests of the Viking decelerator system which were conducted as the Balloon Launched Decelerator Test (BLDT) program at the White Sands Missile Range (WSMR) in the summer of 1972. The prime objective of these tests was to verify the satisfactory operation and performance of the full-scale Viking decelerator in a simulated Mars environment and in the wake of a full-sized Viking entry vehicle. In order to provide the velocity/atmospheric density equivalent of the Mars parachute deployment conditions, the BLDT vehicle was lifted to approximately 120,000 feet in the Earth atmosphere beneath a large balloon system. The BLDT vehicle was similar in size and shape to the Viking entry vehicle. Once at the proper altitude over the White Sands Missile Range, the BLDT vehicle was boosted by rocket motors to the proper test conditions of Mach number and dynamic pressure.

Three test points were originally selected to bracket the range of possible Mars deployment conditions. Test number 1 (vehicle designation AV-1) was to demonstrate performance and structural integrity at deployment conditions that were in excess of the maximum Mars effective dynamic pressure and in excess of Mach number equal to 2.0. The first test vehicle overshot its intended deployment dynamic pressure by about 23 percent because of vehicle damage incurred during launch. Although the parachute was deployed successfully, damage was sustained in two of the gores. The test was subsequently ruled a "no-test" with its objectives reassigned to a fourth test vehicle (AV-4).

Test Number 2 (AV-2) was to demonstrate performance at deployment conditions in the transonic region and at a dynamic pressure lower than could be experienced on Mars.

Test Number 3 (AV-3) was to demonstrate performance at deployment conditions representing a velocity that is less than the Mars envelope and a nominal dynamic pressure.

The four tests were conducted on the dates shown below. Detailed reports on each of these test flights have been published and are referenced. The reader who is interested in more specific information on the launch operations, the BLDT vehicle design and its instrumentation and operational procedures used during the flight is referred to these reference reports:

	Flight Date	Reference Report
AV-1	July 11, 1972	TR-3720289
AV-2	July 26, 1972	TR-3720291
AV-3	August 19, 1972	TR-3720293
AV-4	August 13, 1972	TR-3720295

This report will limit itself to a review of the decelerator performance for the four test flights and will attempt to summarize the status of parachute qualification for the Mars mission.

II. VIKING DECELERATOR SYSTEM

The Viking decelerator is a 53-foot nominal diameter Disk-Gap-Band parachute with dimensions and general arrangement shown in Figure 1. The parachute is fabricated entirely of Dacron Type 52 except for the three-legged bridle which uses a special Goodyear proprietary fiber. The band cloth material is a 1.53 oz/sq yd rip-stop material having a minimum specified strength of 60 lb/in. The disk cloth is a 2.25 oz/sq yd rip-stop material having a minimum specified strength of 104 lbs/in. The minimum specified strength of the radial tapes, circumferential tapes and suspension lines are 900 pounds, 1800 pounds and 880 pounds respectively. The above parachute strength numbers correctly reflect a change made during development to improve the structural integrity of the canopy. The BLDT AV-2 and AV-4 flight test reports erroneously reported the former development strength values.

The parachute is packed in a deployment bag to a density of 43 lbs/ft^3 and stored in a mortar can aboard the BLDT vehicle in much the same manner as the Viking System. At mortar fire, the deployment bag is ejected straight back by a mortar whose reaction force is nominally oriented through the vehicle c.g. A breakdown of the ejected weight is seen in Figure 2 to total 97 lbs. The relative velocity imparted to the deployment bag is expected from ground mortar test experience to be 112 ± 3 FPS.

Additional geometric data on the parachute are tabulated in Table 1.

TABLE 1

PARACHUTE GEOMETRIC PROPERTIES

Item	Relative Value	Value
Nominal diameter	D_o	53 feet
Geometric porosity*	$0.125\ S_o$	276 ft^2
Total area (S_o)**	$(\pi/4)\ D_o^2$	2206.2 ft^2
Disk area+	$0.53\ S_o$	1169.3 ft^2
Disk diameter	$0.726\ D_o$	38.5 ft
Disk circumference	$2.285\ D_o$	121 ft
GAP area	$0.12\ S_o$	264.7 ft^2
GAP width	$0.042\ D_o$	2.2 ft.
Band area	$0.35\ S_o$	772.2 ft^2
Band width	$0.121\ D_o$	6.4 ft
Vent area	$0.005\ S_o$	11.0 ft^2
Vent diameter	$0.07\ D_o$	3.7 ft
Number of suspension lines	--	48
Length of suspension lines	$1.7\ D_o$	90 ft

* Vent plus gap provide 12.5 percent geometric porosity

** Disk + gap + band

+ Includes vent

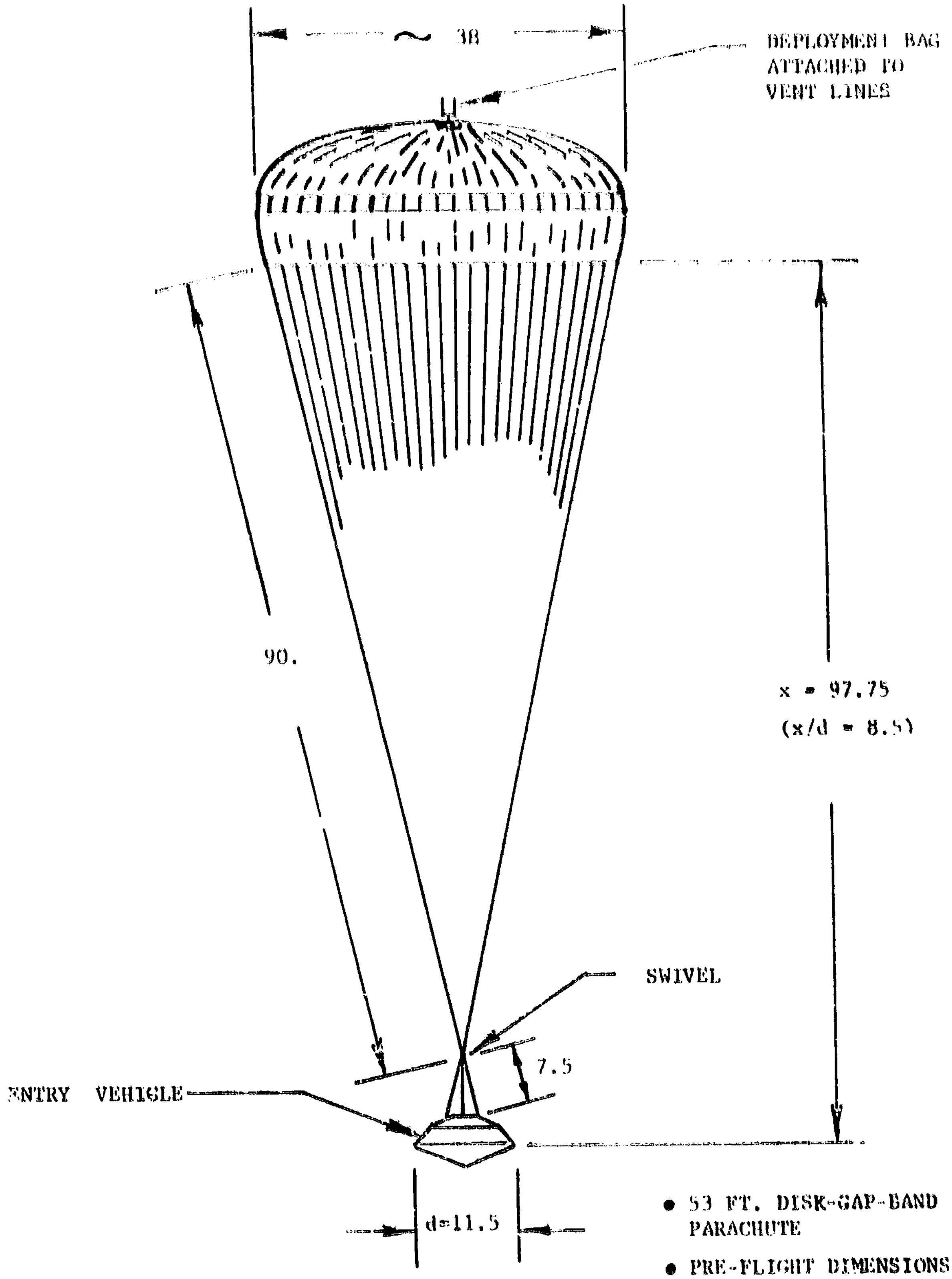

- 53 FT. DISK-GAP-BAND PARACHUTE
- PRE-FLIGHT DIMENSIONS IN FEET

FIGURE 1 VIKING DECELERATOR SYSTEM

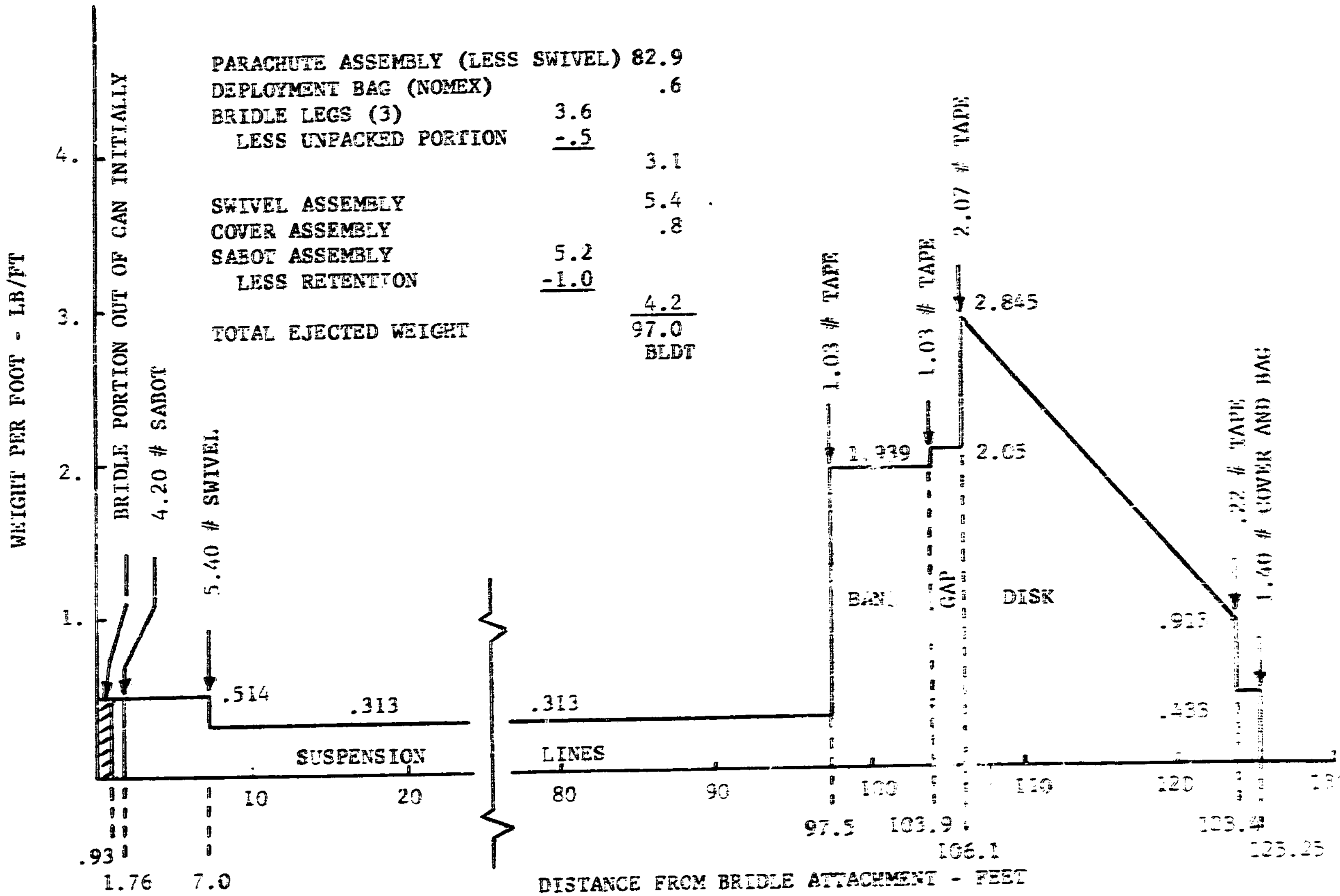

FIGURE 2 EJECTED WEIGHT DISTRIBUTION

III. TEST SYSTEM DESCRIPTION

The desired test conditions of dynamic pressure and Mach number or velocity occur at Earth altitudes in the 140,000 foot altitude range. A combination of balloons and rockets, similar to that utilized for the PEPP tests (Reference 6) were employed to reach the desired test altitude for each test. Four tests were conducted, two at supersonic conditions and one each at transonic and subsonic conditions. The supersonic and transonic tests required propulsion units built into the test vehicle to reach the desired Mach number. The typical powered flight mission sequence is shown in Figure 3. The subsonic test did not need propulsion units, but involved simply a free fall drop from the balloon.

The test vehicle (Figures 4 and 5) was physically similar to the Viking entry vehicle except for the protruding rocket motor nozzles required on the powered vehicles. The test vehicle weighed approximately 1890 lbs at decelerator deployment on each of the flights. On-board instrumentation included forward and aft looking cameras, bridle leg tensiometers, rate gyros and accelerometers. More detailed information on the test system, test system performance and test operations is included in References 2 through 5.

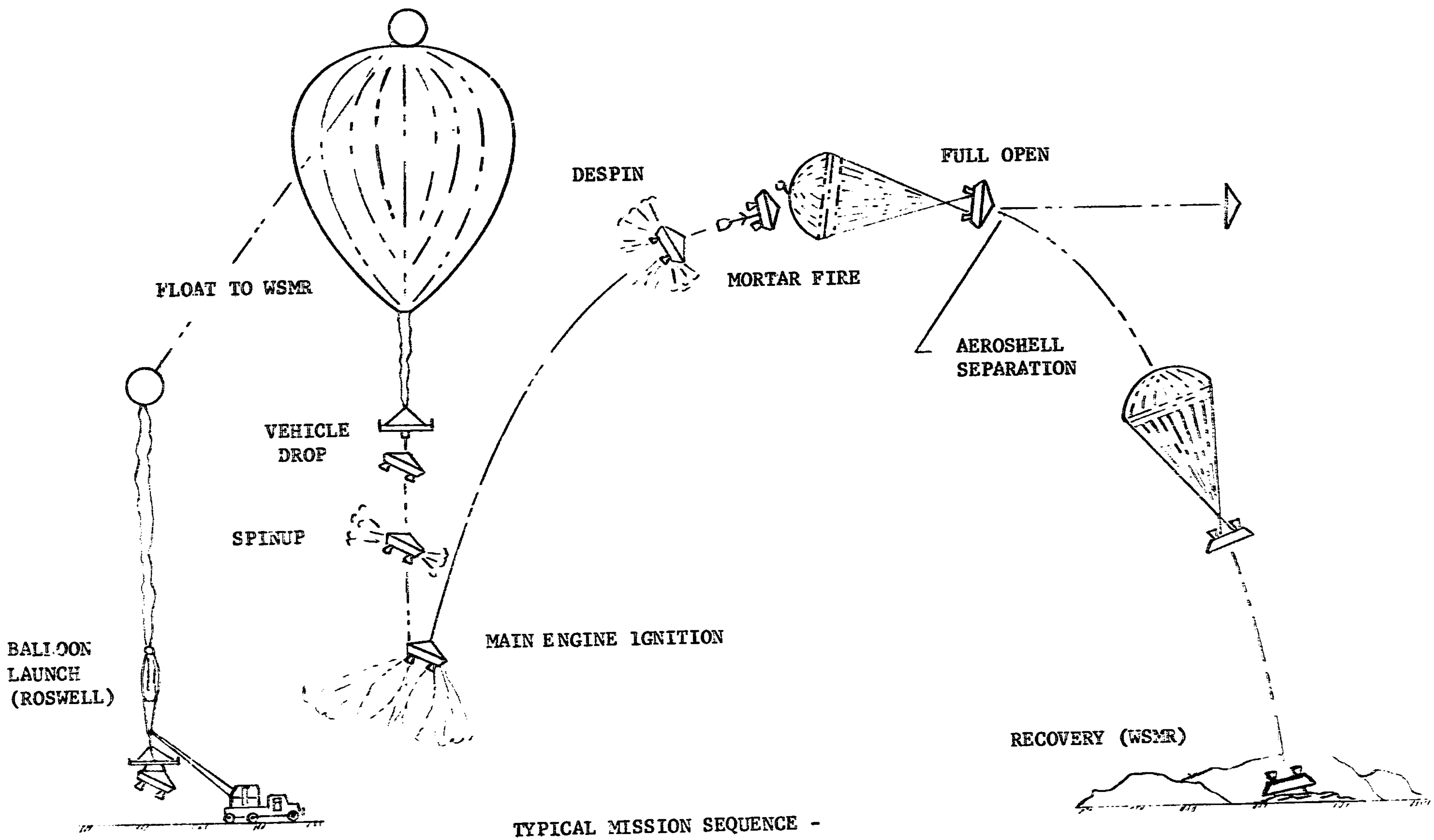

TYPICAL MISSION SEQUENCE -
POWERED FLIGHT

FIGURE 3

(1) -Z AXIS Cg OFFSET = 1.41" ± 0.030"

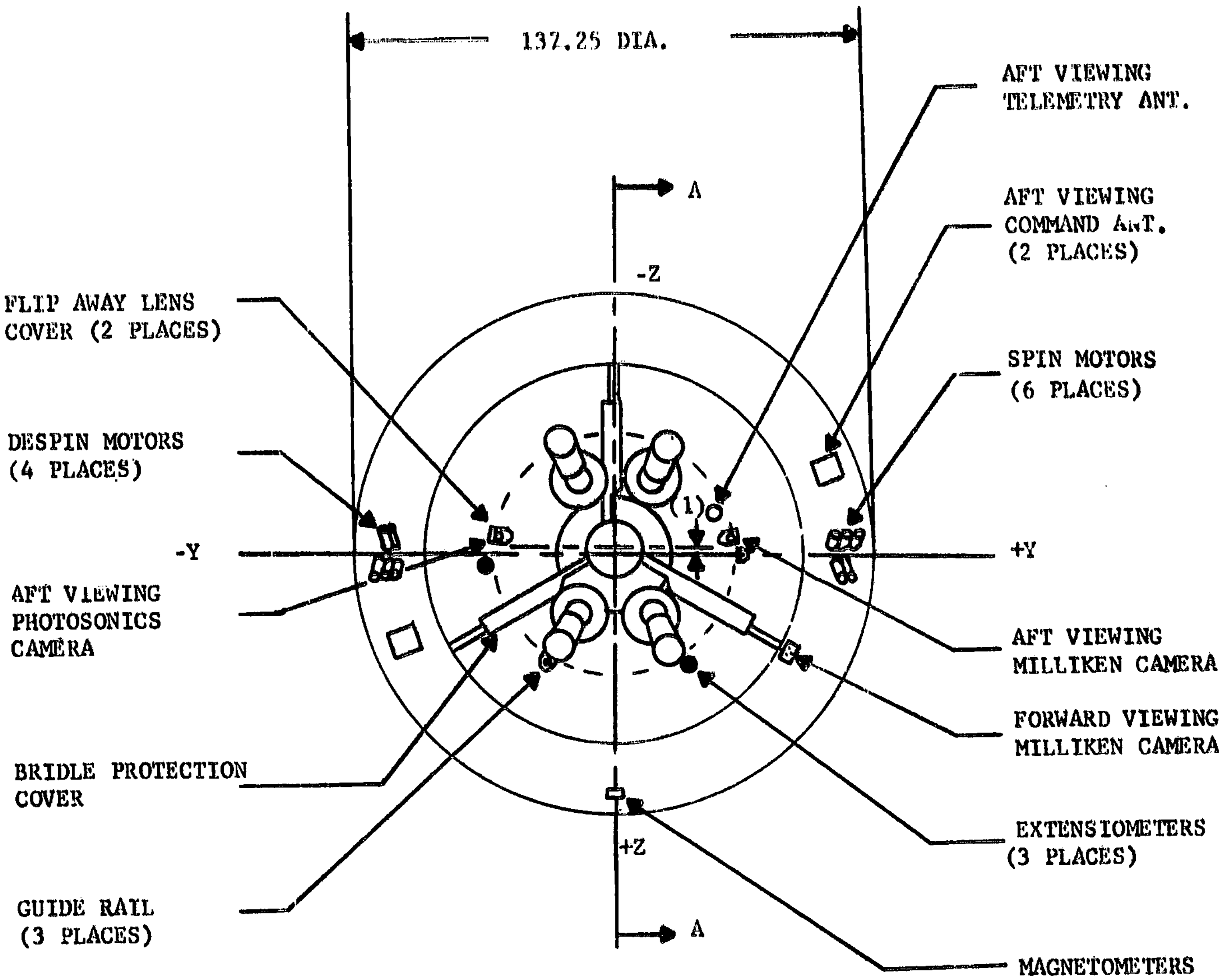

VIEW LOOKING AT AFT END OF VEHICLE

BLDT SUPERSONIC VEHICLE CONFIGURATION

FIGURE 4

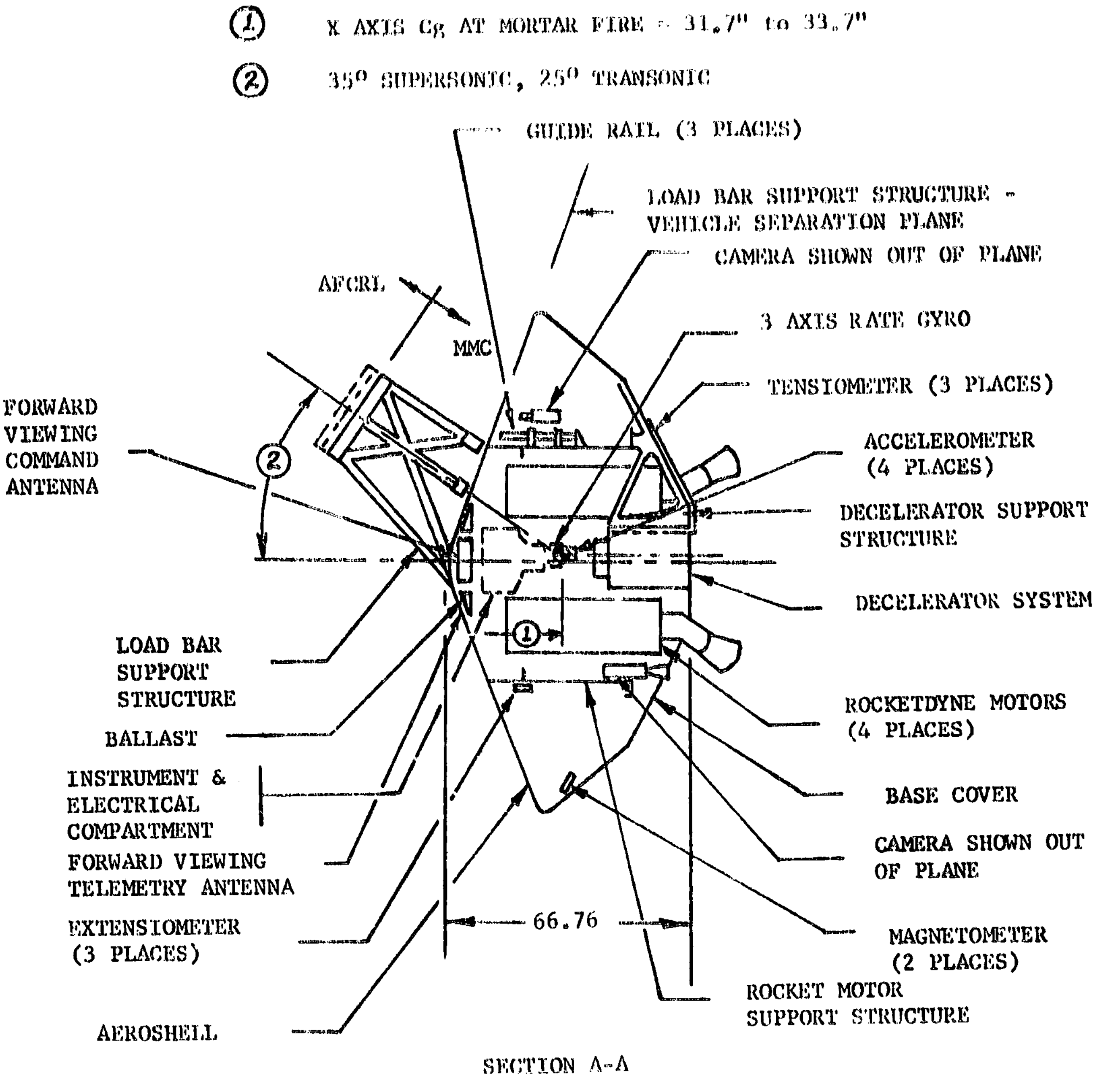

FIGURE 5 BLDT SUPERSONIC VEHICLE SECTIONAL VIEW

IV. MARS QUALIFICATION

A. Test Point Selection

The BLDT test points will bracket the range of possible Mars deployment conditions as indicated in Figure 6.

Test Vehicle AV-1 will demonstrate performance and structural integrity at deployment conditions that are in excess of the maximum Mars effective design dynamic pressure and in excess of Mach 2.0 as in Figure 7.

Test Vehicle AV-2 will demonstrate performance at deployment conditions in the transonic region and at a dynamic pressure lower than the lowest dynamic pressure shown for Mars in Figure 8.

Test Vehicle AV-3 will demonstrate performance at deployment conditions representing a velocity that is less than the Mars envelope shown in Figure 9.

Test Vehicle AV-4 is a re-flight of the maximum Mach and dynamic pressure objectives of AV-1 except that it reflects revised Mars peak load envelope conditions of Figure 10 which were changed as a result of Mariner 9 Mars atmosphere estimates.

B. General Parachute Performance Objectives

The general qualification objectives of all the BLDT flights are:

1. Verify that the mortar provides sufficient velocity to support full deployment of the parachute.
2. Verify that ejection from mortar fire through line stretch, bag strip and initial full inflation is relatively smooth and free of canopy "dumps" or other discontinuities.

3. Verify that canopy maintains a relatively stable drag shape after initial inflation and canopy area oscillation phase is over.

4. Verify that sufficient drag performance is produced to support Viking mission requirements of terminal velocity and aeroshell separation. The drag coefficient produced by the parachute in the presence of the forebody should be within the envelope of C_D versus Mach number as defined in Figure 11. This requirement refers to quasi-steady state drag and does not apply to the highly dynamic pulsations that occur during the parachute opening process.

5. Demonstrate that the parachute has an adequate structural margin to sustain maximum opening loads for the Viking mission and maintain an essentially damage free condition through the deceleration phase.

6. Vehicle oscillations shall be less than or equal to ± 25 degrees amplitude in quasi-steady state descent with no wind when analytically extrapolated to Mars conditions.

7. Vehicle attitude rates shall be less than or equal to 30 degrees/second in quasi-steady state descent with no wind when analytically extrapolated to Mars conditions.

C. Loads Criteria

The critical load test for the parachute is the supersonic case and the objective for this test is to obtain peak load conditions that fall within the Mach number and dynamic pressure envelope defined in Figures 7 and 10. In establishing these load limits, the effective design dynamic pressure for BLDT is adjusted downward to compensate for increased aerodynamic heating and load amplification effects and adjusted upward for the absence of interplanetary cruise degradation. These adjustments are made to compensate for relative changes in the parachute structural capability between BLDT and Mars as follows:

$$q\,[\text{BLDT}] = (W) \cdot (X) \cdot (Y) \cdot (Z) \cdot q\,[\text{Mars design limit}]$$

where:

W = Margin of overtest = 1.3 max.

X = Aerodynamic heating factor = .985

Y = Amplification Effect = .95

Z = Interplanetary Cruise Degradation = 1.03

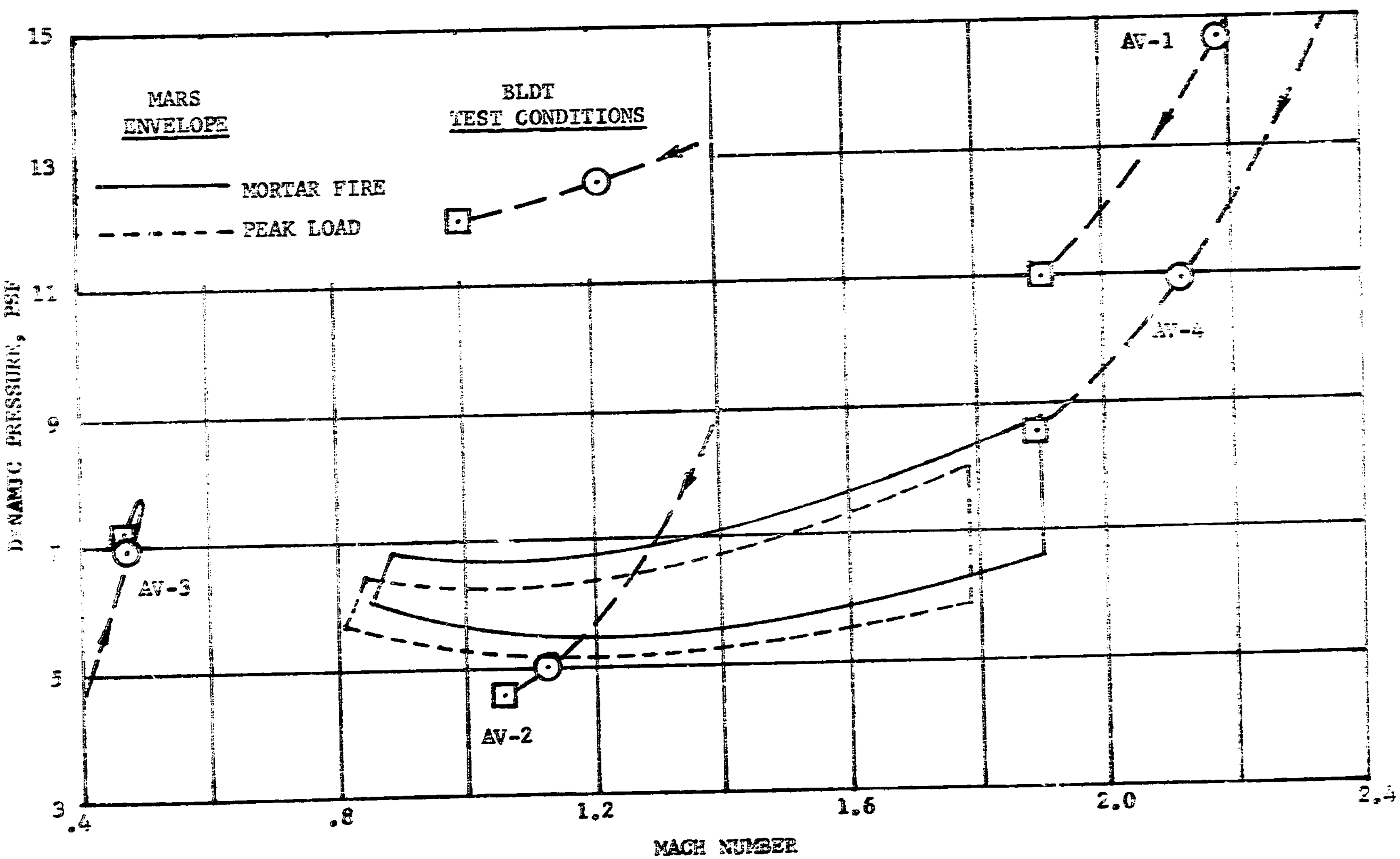

FIGURE 6 MARS ENVELOPE AND TEST CONDITIONS

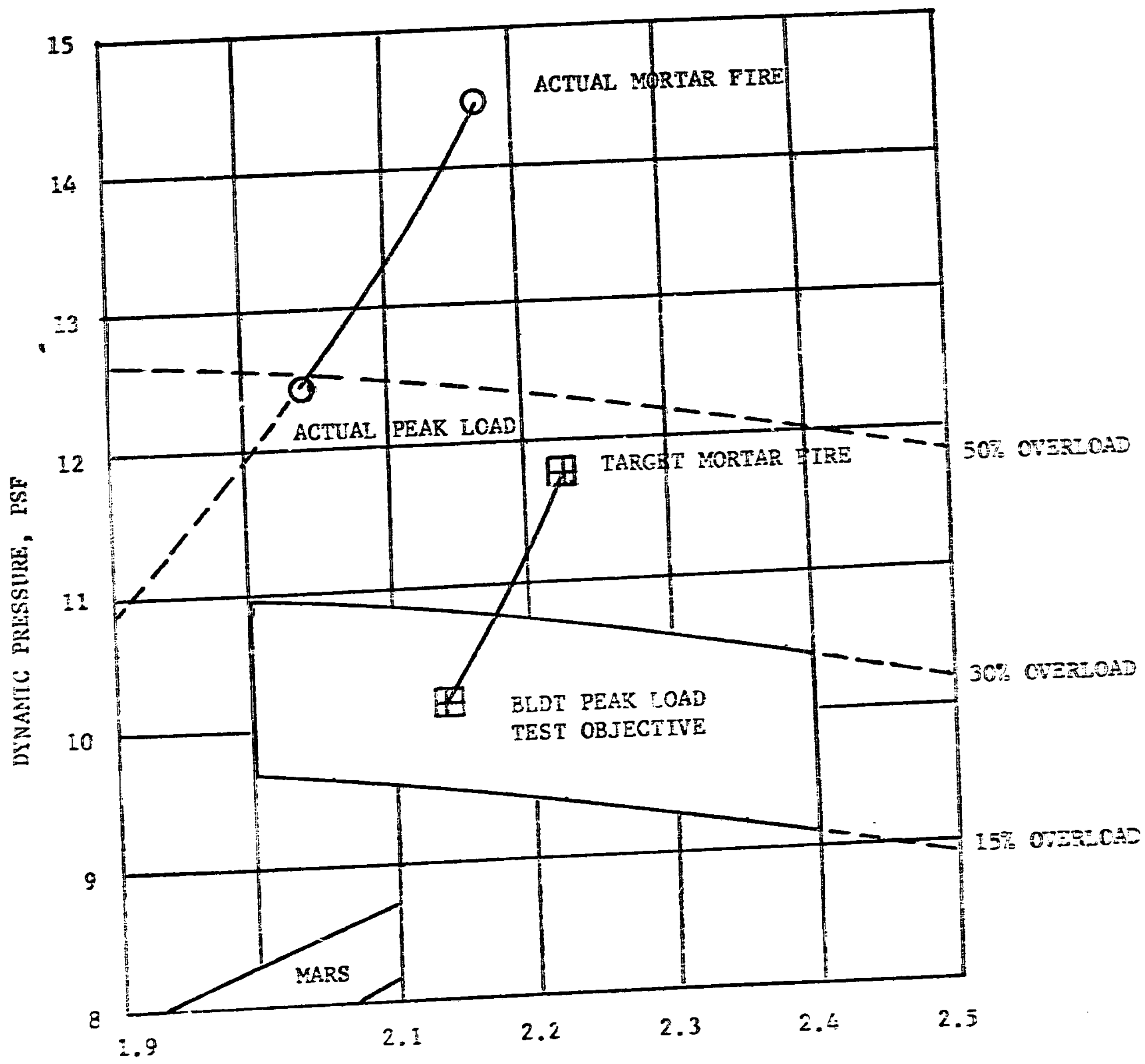

BLDT AV-1 TEST CONDITIONS

FIGURE 7

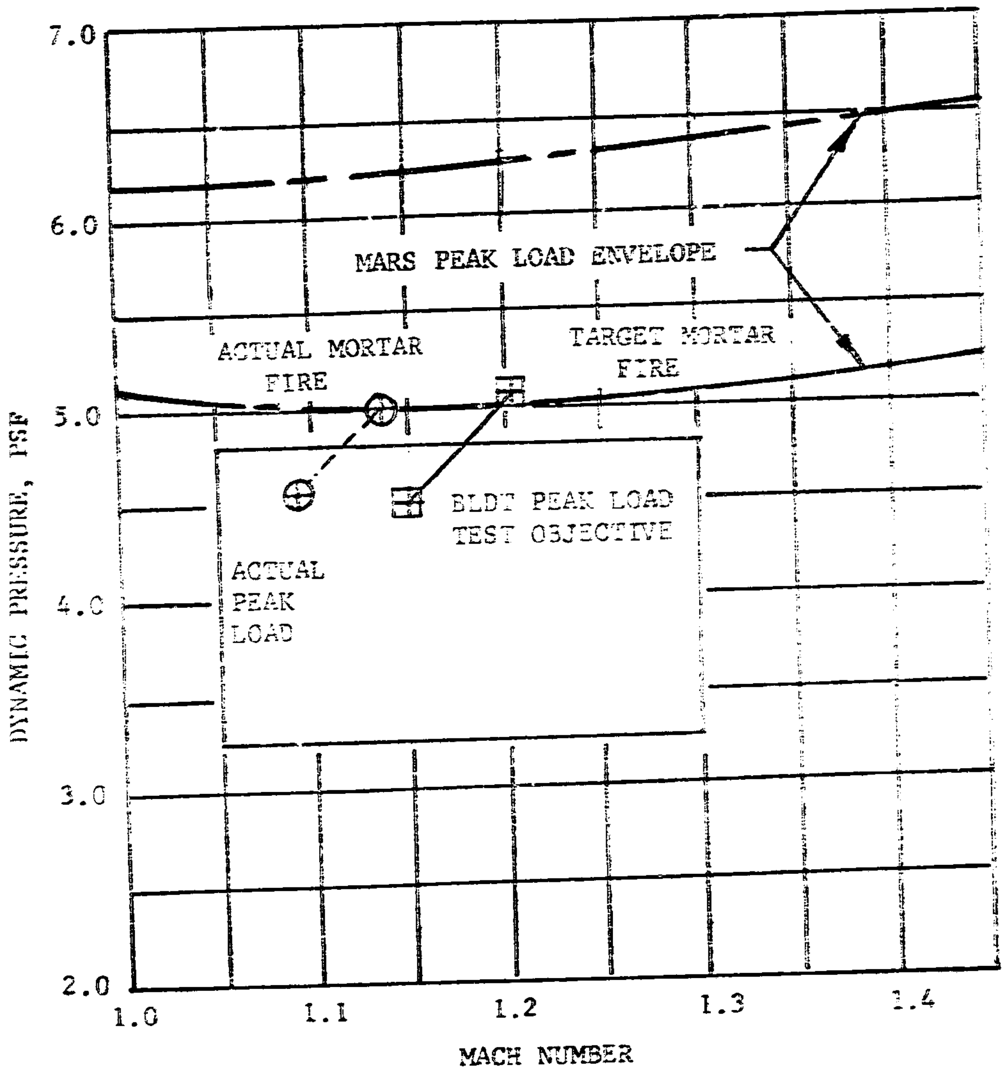

FIGURE 8 BLDT AV-2 TEST CONDITIONS

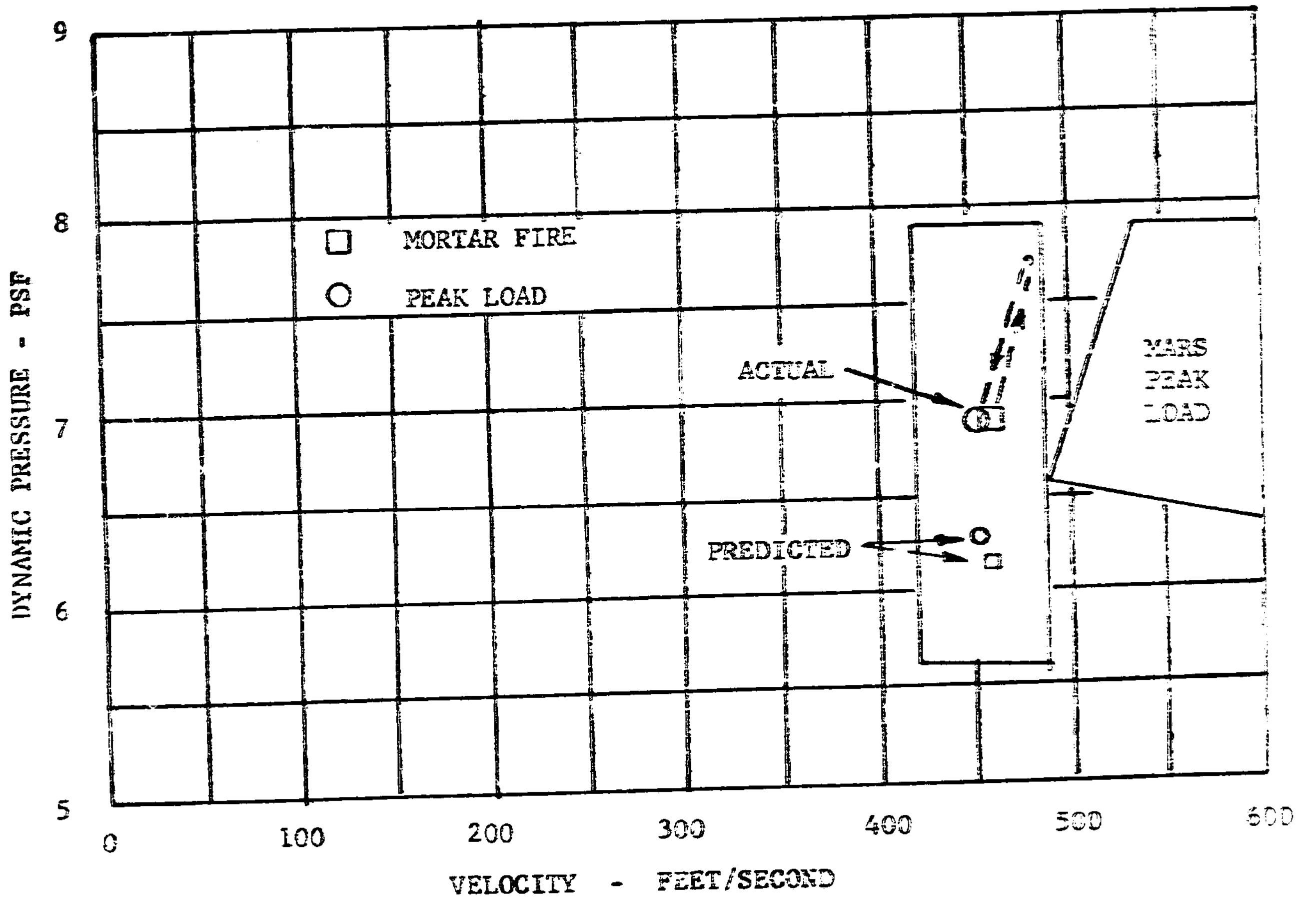

FIGURE 9 BLDT AV-3 TEST CONDITIONS

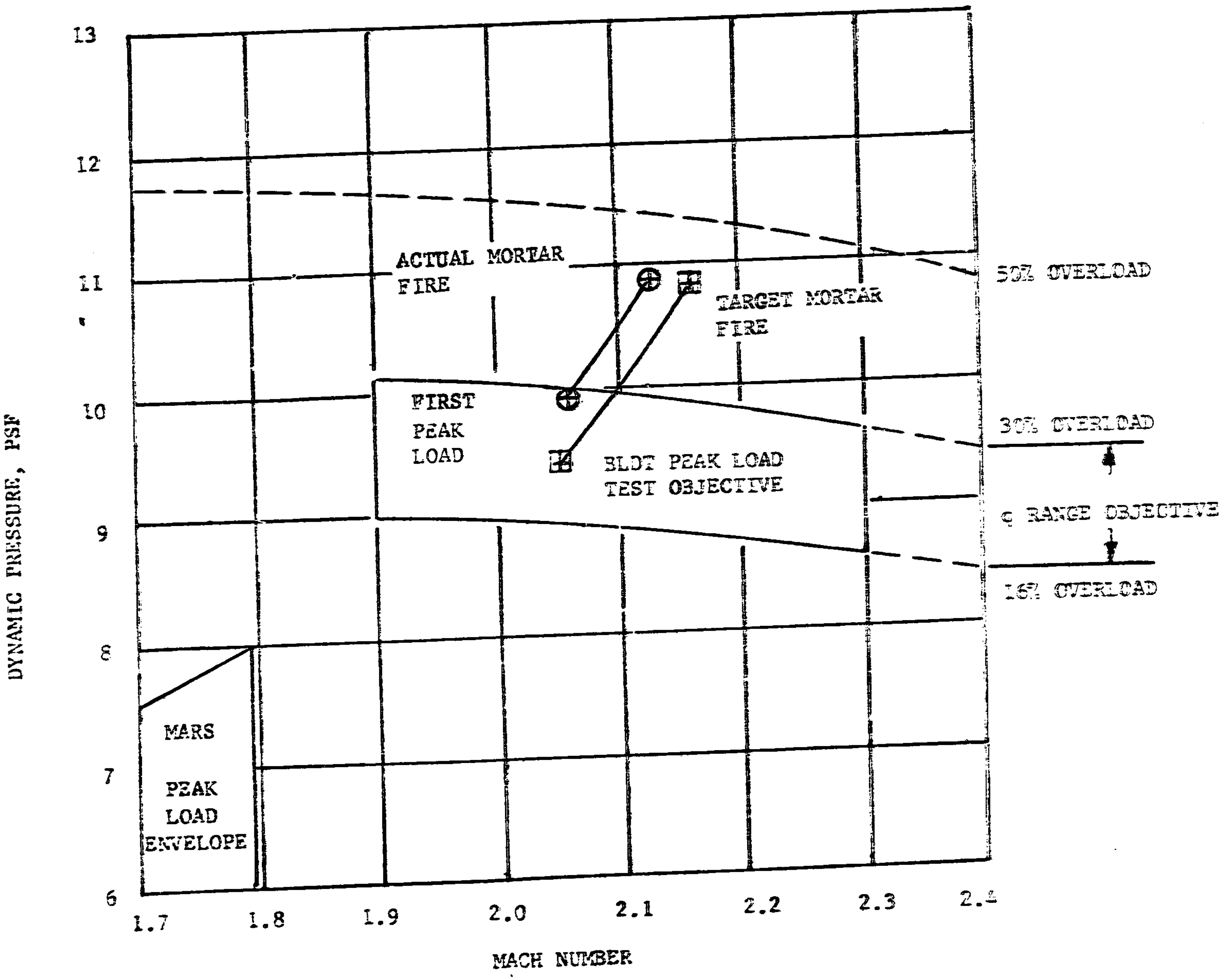

BLDT AV-4 TEST CONDITIONS

FIGURE 10

C_{D_P} = PARACHUTE QUASI-STEADY STATE DRAG COEFFICIENT IN PRESENCE OF FOREBODY

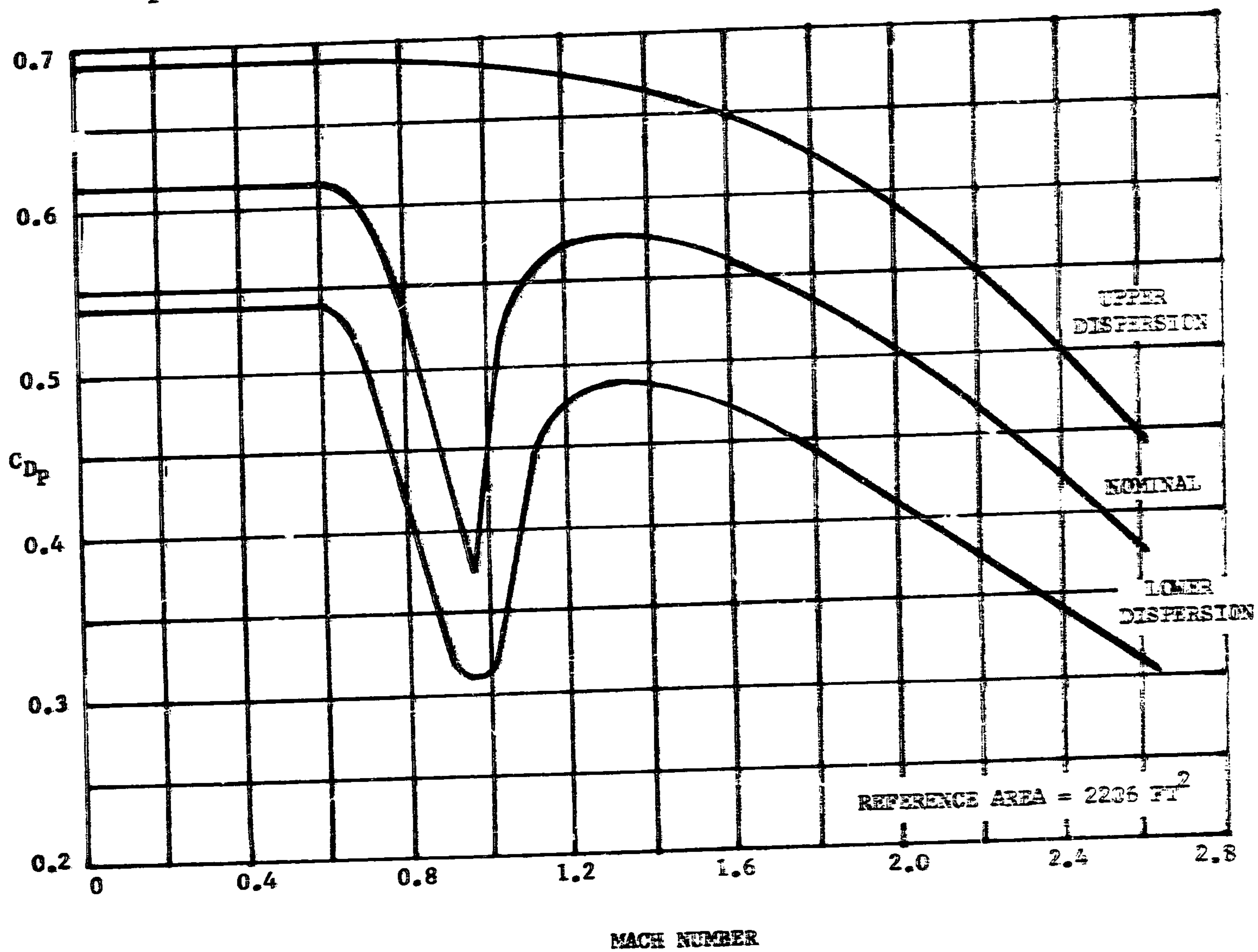

FIGURE 11 PARACHUTE DRAG COEFFICIENT ENVELOPE

V. PARACHUTE DEPLOYMENT CONDITIONS

Parachute deployment conditions on the BLDT flights differ from the Viking conditions in several important respects. The BLDT vehicle had to accept the residual effects of a powered flight phase which included spin-up, despin and main engine thrust tail-off. Secondly, the BLDT vehicle, unlike the Viking entry vehicle, did not have an active attitude control system and could not control attitude rates or angles of attack and sideslip at deployment.

The primary purpose of each BLDT vehicle was to achieve parachute deployment conditions which fell within the desired qualification envelopes discussed in Section IV. This was accomplished for each test condition by selecting the proper drop attitude from the balloon, choosing the number and type of rocket motors for the desired thrust and firing the mortar either by ground command or by airborne timer. Within these design constraints the actual deployment conditions were further influenced by numerous flight performance dispersions which were to some degree predictable but had to be controlled as tightly as possible.

A summary of actual parachute deployment conditions achieved on each of the BLDT flights is presented in Table 2.

TABLE 2

BLDT PARACHUTE DEPLOYMENT CONDITIONS

	AV-1	AV-2	AV-3	AV-4
Mach Number	2.18	1.133	.47	2.126
Dynamic Pressure, psf	14.63	5.00	6.9	10.90
Velocity, FPS	2314	1194	464	2290
Axial Acceleration, G's	- 1.18	- .40	- .34	- .93
Altitude, Feet	142025	135368	87027	147186
Angle of Attack, degrees	- 12	5.4	3.5	- 4.1
Angle of Sideslip, degrees	- 2	- 4.9	- 4.5	- 3.1
Total Angle of Attack, degrees	13	7.28	5.7	5.2
Parachute Temperature, ^{o}F	50	47	26	46
Residual Spin Rate, deg/sec	- 26	- 62	- .5	- 30
Pitch Rate, deg/sec	2	13	2.1	- 14
Yaw Rate, deg/sec	- 3	3	- 5.8	4
Trim Angle of Attack, degrees	- 8.5	- 3.7	- 4.3	- 9.
Deviation from Trim, degrees	4.	10.4	9.1	6.

The actual deployment conditions are compared to the qualification envelopes in Figures 7, 8, 9 and 10. Examination of these figures reveals that with the exception of AV-1 which was subsequently ruled a "no test", all flight test peak load points fell within the desired qualification envelopes. In some cases, such as AV-3 (Figure 9), deviation in the planned drop altitude accounted for much of the difference between targeted and actual deployment conditions. An overview of all the test points plotted with relation to the latest Mars envelope in Figure 6 shows that the decelerator has truly been tested at conditions that encompass upper and lower limits of Mach number and dynamic pressure.

A review of some of the other deployment conditions from Table 2 reveals additional qualification data. The maximum BLDT total angle of attack of 13 degrees compares favorably with the Mars nominal trim condition of 11.9 degrees at Mach 2.0. Stowed parachute temperature conditions on all flights were lower than the 8C°F requirement to limit aerodynamic heat degradation of the canopy at the higher Mach number conditions.

The attitudes and attitude rates for BLDT are indicative of vehicle dynamic motions which are significantly higher than what is expected on Mars. An indication of how far each vehicle was away from its trim condition at deployment is obtained by computing the vector difference between total angle of attack at deployment and at aerodynamic trim. This vector difference, shown as deviation from trim in Table 2 was as high as 10.4 degrees on BLDT whereas the Viking vehicle oscillation about trim is expected to be ±3 degrees (Reference 17). Attitude rates as high as 14 degrees/second on BLDT compare with Viking rates that are controlled by an attitude control system to approximately 1 degree/second.

VI. MORTAR PERFORMANCE

The minimum mortar velocity required for the Viking decelerator was established by requiring a positive velocity margin of at least 5 FPS at bag strip under the most adverse deployment conditions. The Viking entry vehicle is decelerating at 23 ft/sec^2 in the worst case at parachute deployment. Additional assumptions used in establishing a minimum mortar velocity are:

1. The maximum ejected weight is 100 lbs.
2. The deployment bag drag is zero during canopy and line strip. This assumption more than adequately accounts for dynamic pressure degradation behind the blunt aeroshell.
3. Line stripping friction is assumed to be a constant value of 2 lbs. (Ref. 8).
4. Canopy stripping friction is assumed to be a constant value of 6 lbs. (Ref. 8)
5. A 2-body ejection simulation method (Ref. 9) is used which considers variable mass distribution and momentum exchange between deployment bag and lander.

The minimum Viking mortar performance defined by the above conditions is 94 FPS (Ref. 7). On the supersonic BLDT flight tests (AV-1 and AV-4) where a 1.3 overload in dynamic pressure is targeted, the increased BLDT deceleration adds approximately 10 FPS to the mortar velocity requirement for equivalence between BLDT and Viking during the bag strip process. A mortar design was chosen which had the additional margin of ejection velocity to make it suitable for both BLDT and Viking. Mortar development tests (Ref. 8) conducted in a chamber where altitude and temperature could be simulated showed a mean mortar velocity of 110.6 FPS with a standard deviation of 4.42 FPS.

Actual BLDT mortar performance is evaluated by observing the bag stripping process from on-board cameras. When the suspension lines are fully payed out of the deployment bag, line stretch occurs and the canopy starts emerging from the bag. This event causes an identifiable spike to occur on the telemetered tensiometer loads and can readily be identified on the on-board film. The time from mortar fire to line stretch is therefore accurately determined. The actual distance the deployment bag must travel for the suspension lines to be pulled from the bag is defined by the length of the lines themselves. For most of the low dynamic pressure applications that are typical of the Mars deployment, the lines may be assumed to follow a straight line between lander and the bag. For higher dynamic pressure and angle of attack conditions such as were experienced on AV-1, a line bowing correction was applied to account for the aerodynamic influence on the lines. By simulating the mortar firing process with complete aerodynamic forces and momentum exchange between the forebody and the deployment bag, a mortar velocity can be deduced. A summary of the mortar performance determined from a review of the flight data and simulation is presented in Table 3.

TABLE 3

BLDT MORTAR PERFORMANCE

	AV-1	AV-2	AV-3	AV-4
Mortar Velocity, FPS	112	106.5	106	114.2
Time to Line Stretch, Sec.	1.03	1.015	1.02	.99
Relative Velocity at Line Stretch	72	92.6	91.8	86.4
Time to Bag Strip, Sec.	1.40	1.31	1.32	1.30
Relative Velocity at Bag Strip	71.5	83.9	84.3	83.6

All the BLDT flight mortar velocities exceed the minimum Viking requirement of 94 FPS and show a substantial relative velocity remaining at bag strip to assure positive bag strip. There appears to be a fair amount of variation in mortar velocity from flight to flight. If we combine all the ground and flight mortar data of a common design, the mean mortar velocity is 110 FPS with a standard deviation of 4.0 FPS. The chance of the mortar velocity being as low as 94 is seen to be extremely remote.

VII. PARACHUTE INFLATION CHARACTERISTICS

The on-board Milliken and Photosonics aft-viewing camera films were examined in detail to establish event times and to document the character of the parachute inflation. Filling times from either line stretch or bag strip are summarized in Table 4.

Table 4

Parachute Inflation Characteristics

	AV-1	AV-2	AV-3	AV-4
Filling Time from Line Stretch, sec.	.56	.64	.81	.56
Filling Time from Bag Strip, sec.	.25	.35	.52	.312
Vehicle Velocity at Line Stretch, fps	2250	1160	459	2245
Vehicle Velocity at Bag Strip, fps	2218	1150	458	2235

The filling times for the BLDT flights are plotted in Figure 12 along with flight test data from the low altitude bomb drop development tests and Planetary Entry Parachute Program (PEPP) results (Reference 10). The data which uses bag strip as a zero reference more nearly reflects classical filling time since less than 10 percent inflation occurs before bag strip. The handbook design filling time equation for parachutes with inherent geometric porosity ($t_f = .65 \cdot \lambda_G \cdot D_o/V$ - Reference 11) agrees reasonably well with the Viking parachute test data in Figure 12. The envelope of test data thus established provides good assurance that large uncertainties in filling time are unlikely.

The growth of the canopy from line stretch was obtained by integrating the projected area images from the Milliken camera. A canopy growth parameter curve of normalized area versus time for each parachute test is included in Figure 13. The projected area at any time is divided by the projected area in the final seconds of airborne film coverage (50 seconds after mortar fire). The time scale is normalized by the total filling time. Comparison of the BLDT canopy growth curves shows them all to be well behaved and very similar. The curve for AV-1, as might be expected, showed the effect of a damaged canopy by deviating most significantly from the others. That part of the inflation curve from bag strip to full open is seen to be approximated very closely by a cubic function of time.

After first full inflation the canopy typically goes through a short period of unstable inflation shown in Figure 14. The BLDT canopy behavior is very similar to that shown on previous Disk-Gap-Band tests in the PEPP series, and like PEPP showed increased instability at the supersonic deployment conditions. Two dips in projected area, one at 2.0 seconds on AV-2 and another at 2.5 seconds on AV-4 are more pronounced than previously seen on PEPP. These appear to be caused by the canopy moving across the wake of the blunt forebody which unlike PEPP remained in place after parachute deployment. After the short period of area oscillations shown in Figure 14, the canopy achieved steady inflation and remained stable thereafter. No correction has been applied to the parachute projected area ratio to account for variation in the canopy image plane under changing load conditions.

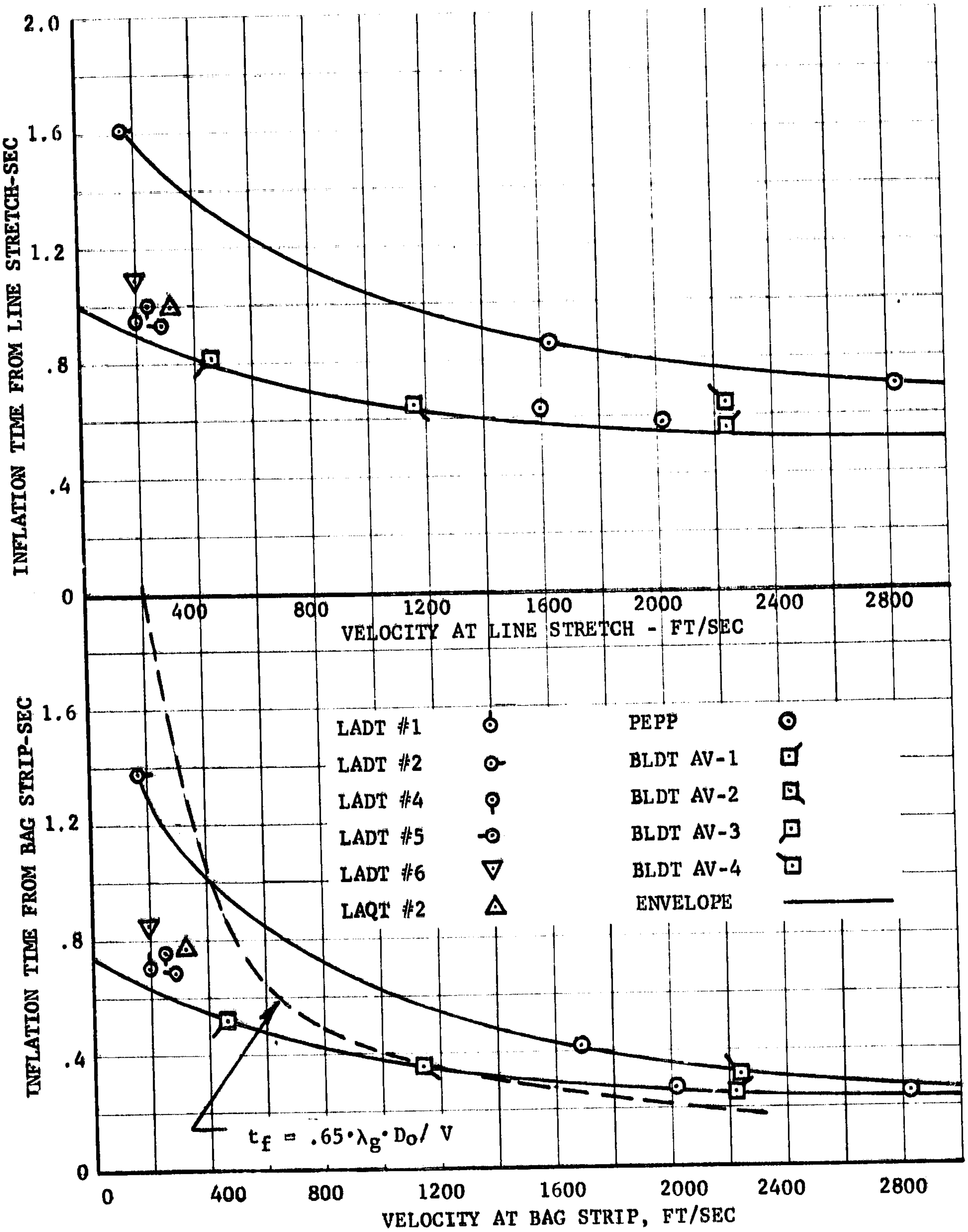

FIGURE 12 PARACHUTE FILLING TIME DATA

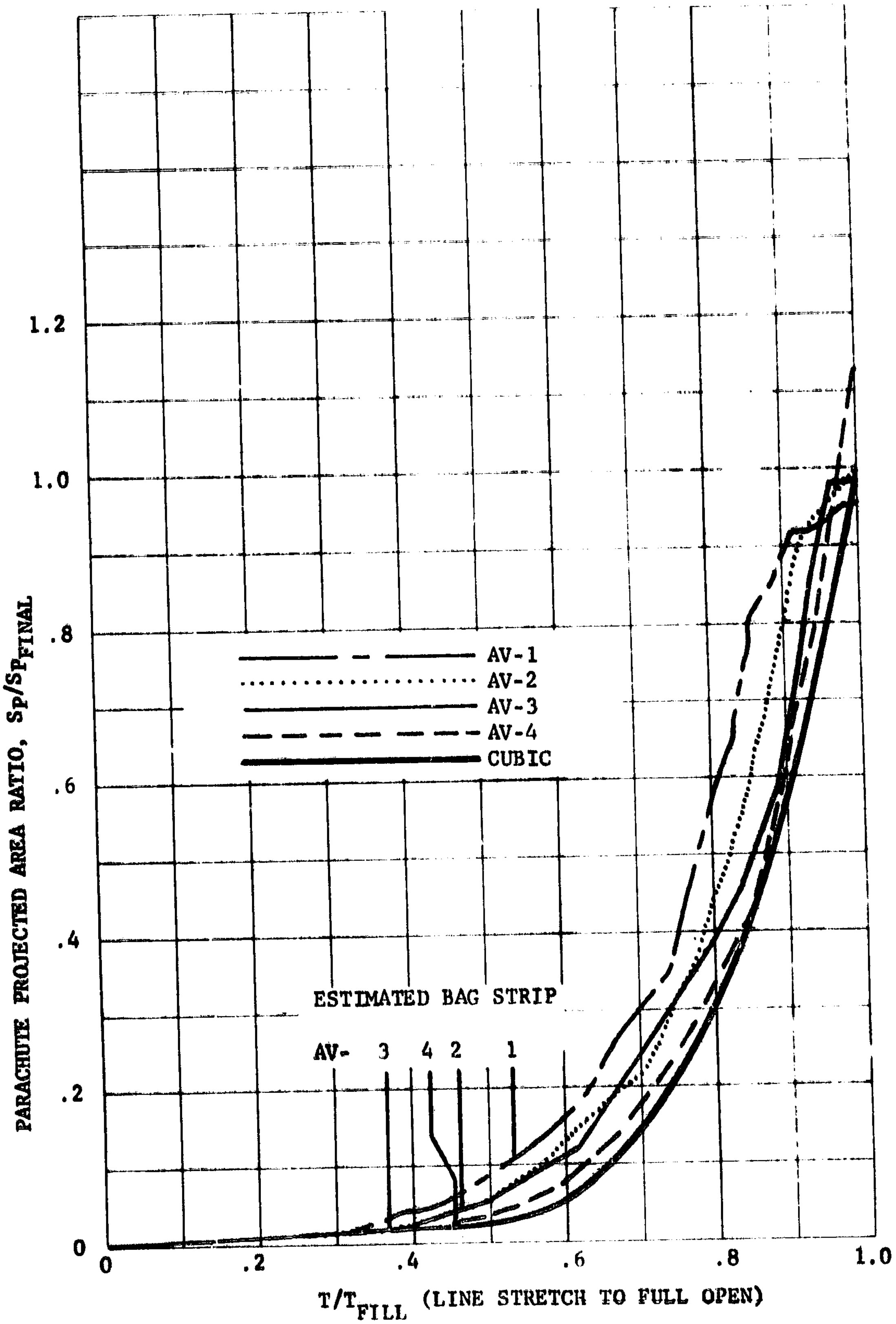

FIGURE 13 CANOPY GROWTH PARAMETER

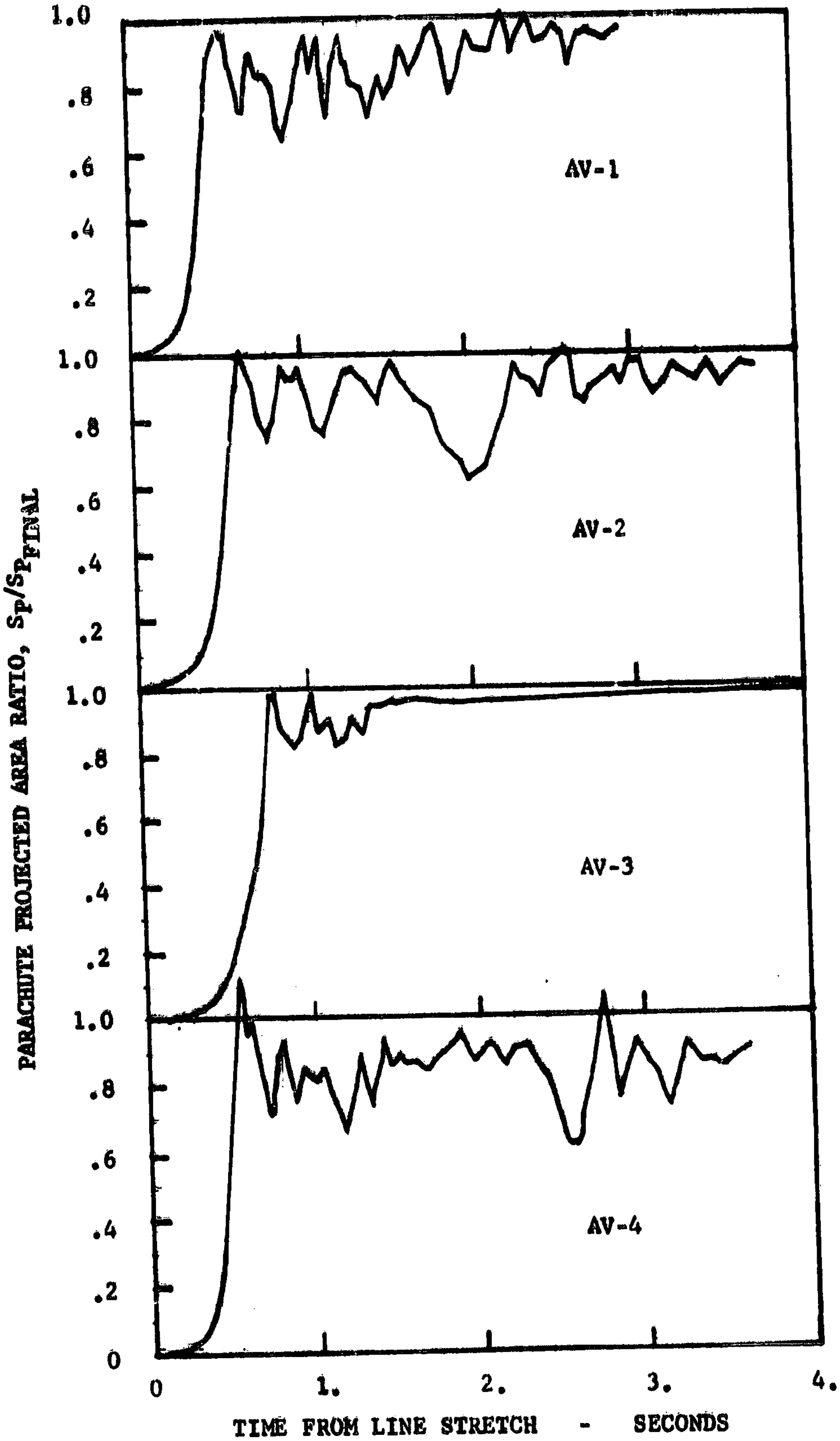

FIGURE 14 CANOPY AREA OSCILLATIONS

VIII. OPENING LOAD AND PREDICTION METHODS

Opening load prediction has made rapid strides in recent years with the aid of high speed digital computers. The work of Heinrich (Reference 12), Berndt and DeWeese (Reference 13) and Toni (Reference 14) have contributed notably towards an understanding of the parachute opening load problem. In spite of all this progress, opening load prediction is still very difficult because the non-rigid structure is made of textiles with complex visco-elastic properties. General practice has been to verify the analytical predictions with load factors determined from full scale tests. The Viking problem, however, involves an atmosphere which we cannot simulate very well here on Earth. We are dependent therefore upon our simulation tools for Mars opening load prediction. Part of the qualification process, then, is to compare our predicted opening loads with the actual BLDT results and from this comparison to make an assessment of how well we can predict Mars opening loads.

Although it is beyond the scope of this discussion to go into the details of our opening load prediction methods, a few points can be made. The methods used represent the joint efforts of Goodyear Aerospace (GAC). Langley Research Center (LRC) and Martin Marietta Corporation and therefore consider most of the usual state-of-the-art features. Of particular concern on the Viking application are the blunt forebody effects on the parachute drag coefficient. Wind tunnel data (Reference 15) shown in Figure 15 show a dramatic difference between chute alone drag and drag in the wake of the Viking lander. The difference has been attributed to mutual interference effects between parachute and forebody. For the purpose of opening load determination, the chute alone data has been used on the assumption that interference drag losses take a finite length of time to be established after first inflation. The assumed value of drag coefficient used in load prediction may, of course, be reviewed to incorporate BLDT test results.

Load/elongation testing of the Dacron 52 suspension line material has revealed some interesting properties. First, stress/strain curve non-linearities have led us to include these effects in our simulation model rather than using a simple spring constant. Secondly, testing of the suspension lines at different load onset rates has revealed a strong sensitivity to this effect. The lower load/elongation curve in Figure 16 was obtained where the strain rate was 1.67 percent per second. The upper curve was generated by a strain rate of 100 percent per second. It became apparent that the difference between the upper and lower curve simply reflected viscous damping and could be related to the relative velocity between lander and parachute during the inflation process. Another interesting property of textiles is the change in apparent elastic properties after peak load during the unloading cycle as noted in Figure 16. This hysteresis effect is time dependent and results in permanent deformation when the load is removed.

The parachute opening loads experienced on BLDT are recorded by tensiometers in each of the three bridle legs and by on-board accelerometers. The tensiometers are summed directly to obtain the total parachute load whereas the accelerometer readings include aeroshell drag which must be subtracted out to obtain parachute loads. The conditions at peak load are summarized in Table 5.

Table 5

BLDT PEAK LOAD CONDITIONS

	AV-1	AV-2	AV-3	AV-4
Mach Number	1.91	1.06	.46	1.89
Dynamic Pressure, psf	11.00	4.55	7.18	8.50
Peak Axial Acceleration, G's	-11.2	-5.62	-7.86	-9.728
Peak Load (Tensiometer), lbs.	17393	9009	12906	16196
Peak Load (Accelerometer), lbs.	18260	9408	13400	16050
Predicted Load for above conditions, lbs.	19500	7029	12558	17123
Effective Drag Coefficient, F/qS	.717	.897	.815	.863
Filling Time from Line Stretch, sec	.56	.64	.81	.56

One must keep in mind that the opening loads recorded by the tensiometers or the accelerometers can be in error by as much as 5 percent. A comparison of the actual versus predicted load data in Figure 17 shows the in-flight measurements, however, agreeing reasonably well with each other. The predicted loads, on the other hand, seem to show a systematic error band which underpredicts at low load and overpredicts at high loads. This is a more desirable situation than the other way around and may simply reflect undue conservatism that creeps into worst case analyses. There are several other possible explanations, however, that seem more likely. The phase relationship between load application and the natural frequency of the system may be different in reality than in the model. This is the old problem that shows up occasionally even in two tests at identical dynamic pressure because no two inflations are the same dynamically. Another explanation for the error band may lie in our assumed load/elongation and damping properties shown in Figure 16. This is suggested by the shape of both the actual and predicted load curves in Figure 17. Note the upper bend in the curves appears at a single line load level of 330 lbs. which is where the 100 percent strain rate curve bends also. Indeed, if we plot the elastic portion of the opening load from our simulation in Figure 17 it resembles the shape of the actual load more closely than the simulation total load which includes damping. This may imply that the shape of our assumed damping curve is in error. This last explanation seems to be the most reasonable and suggests an adjustment of our model to more nearly agree with BLDT results.

Even with no modification to our load prediction model, the BLDT results imply that we will certainly be able to predict the Mars opening load for a given set of conditions to within ±2000 lbs. At the Mars maximum predicted load level of 13500 lbs., the uncertainty in load prediction will be closer to ±1000 lbs. and we will more likely overpredict than underpredict.

Since the character of an opening load curve is often of interest, the BLDT opening load curves are presented in Figures 18, 19 and 20.

One of the benefits of having individual load cells at each of three bridle legs, is the ability to determine the pull angle that the parachute load makes with the longitudinal axis of the vehicle. The value most significant for structural design purposes is the pull angle value occurring at peak load. This value was amazingly consistent on BLDT in spite of the wide variety of deployment conditions. The four flight values were 3.0 (AV-1), 3.0 (AV-2), 3.5 (AV-3), and 3.2 (AV-4) for an average of 3.17 degrees.

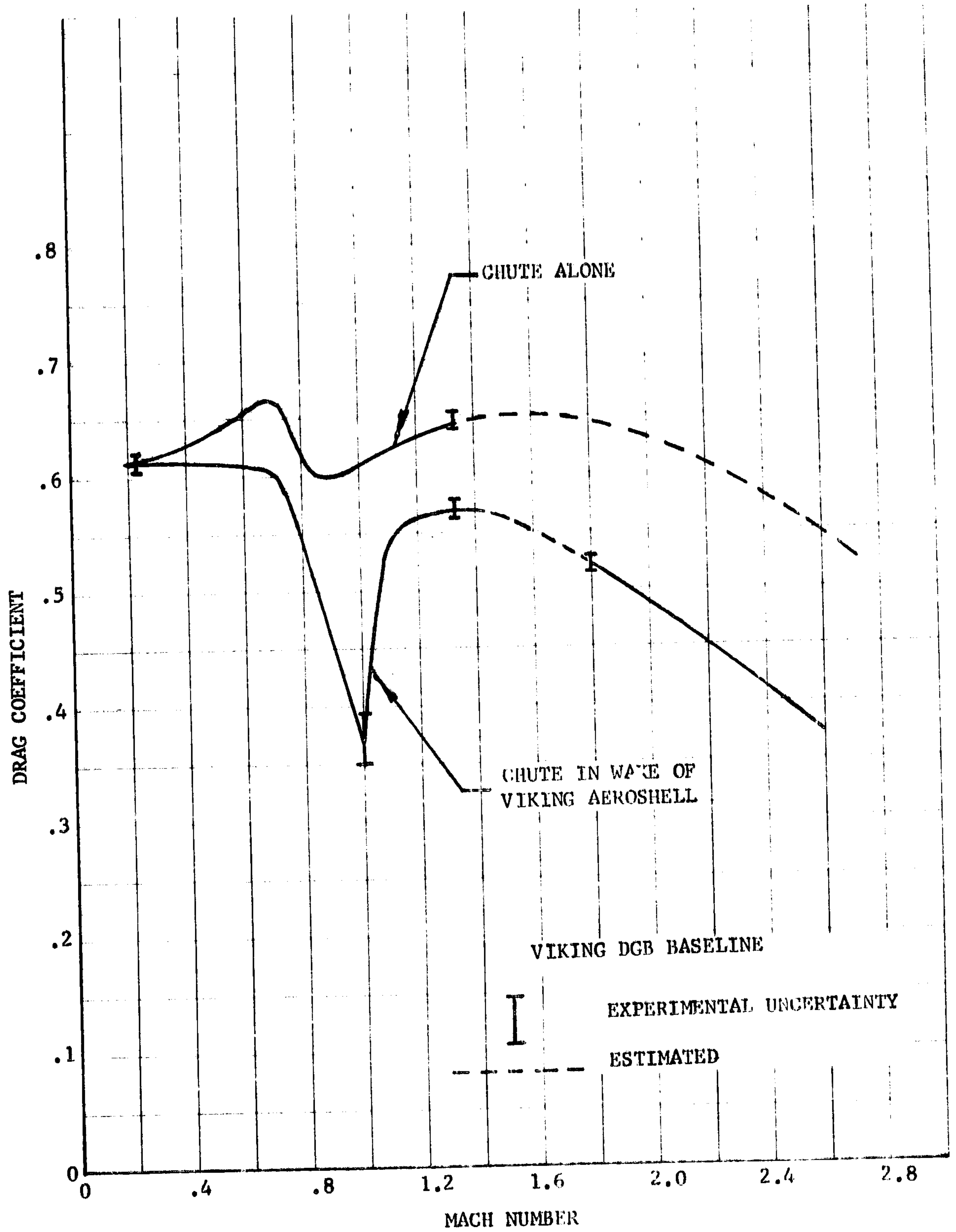

FIGURE 15 WIND TUNNEL DRAG DATA

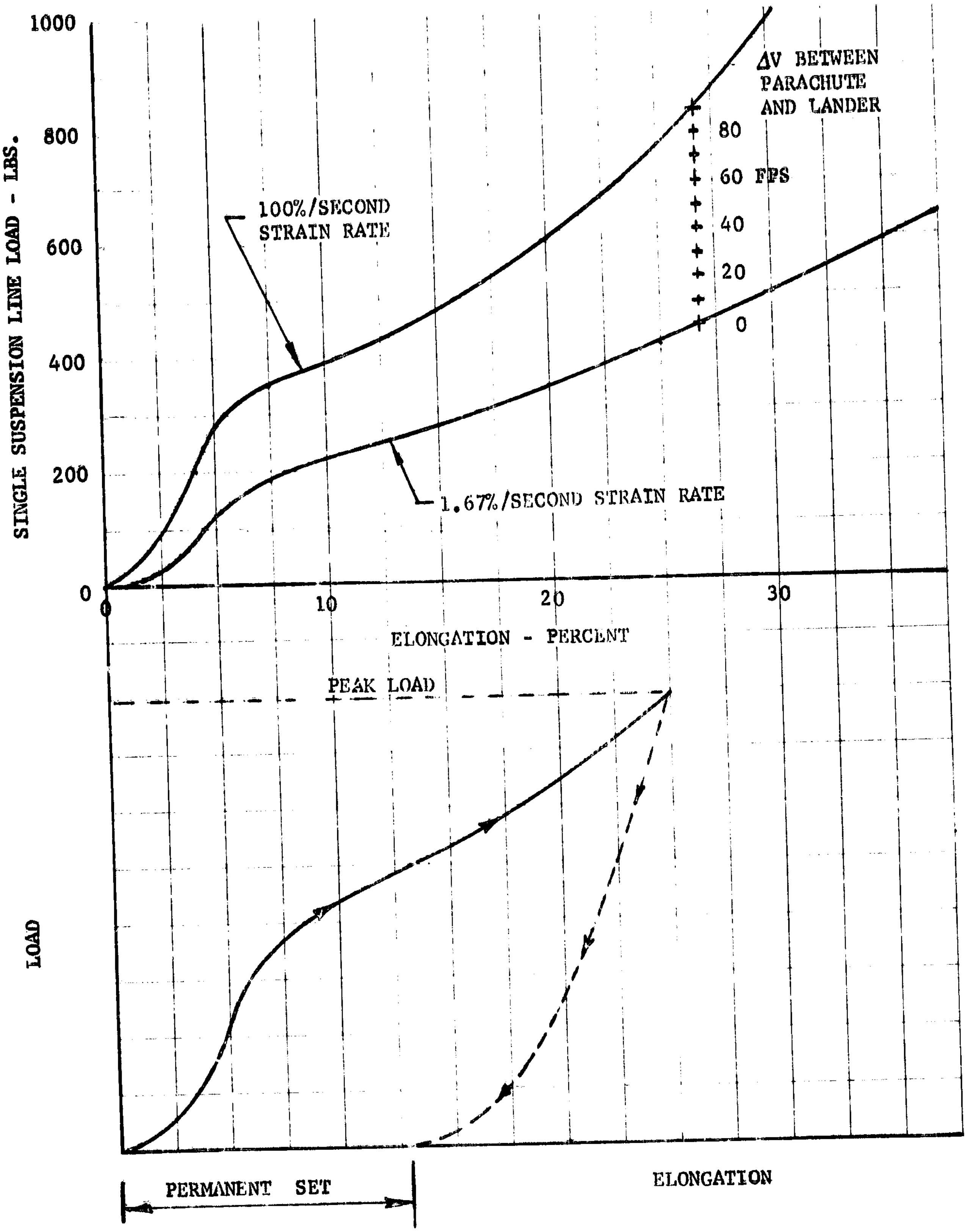

FIGURE 16 SUSPENSION LINE LOAD/ELONGATION DATA

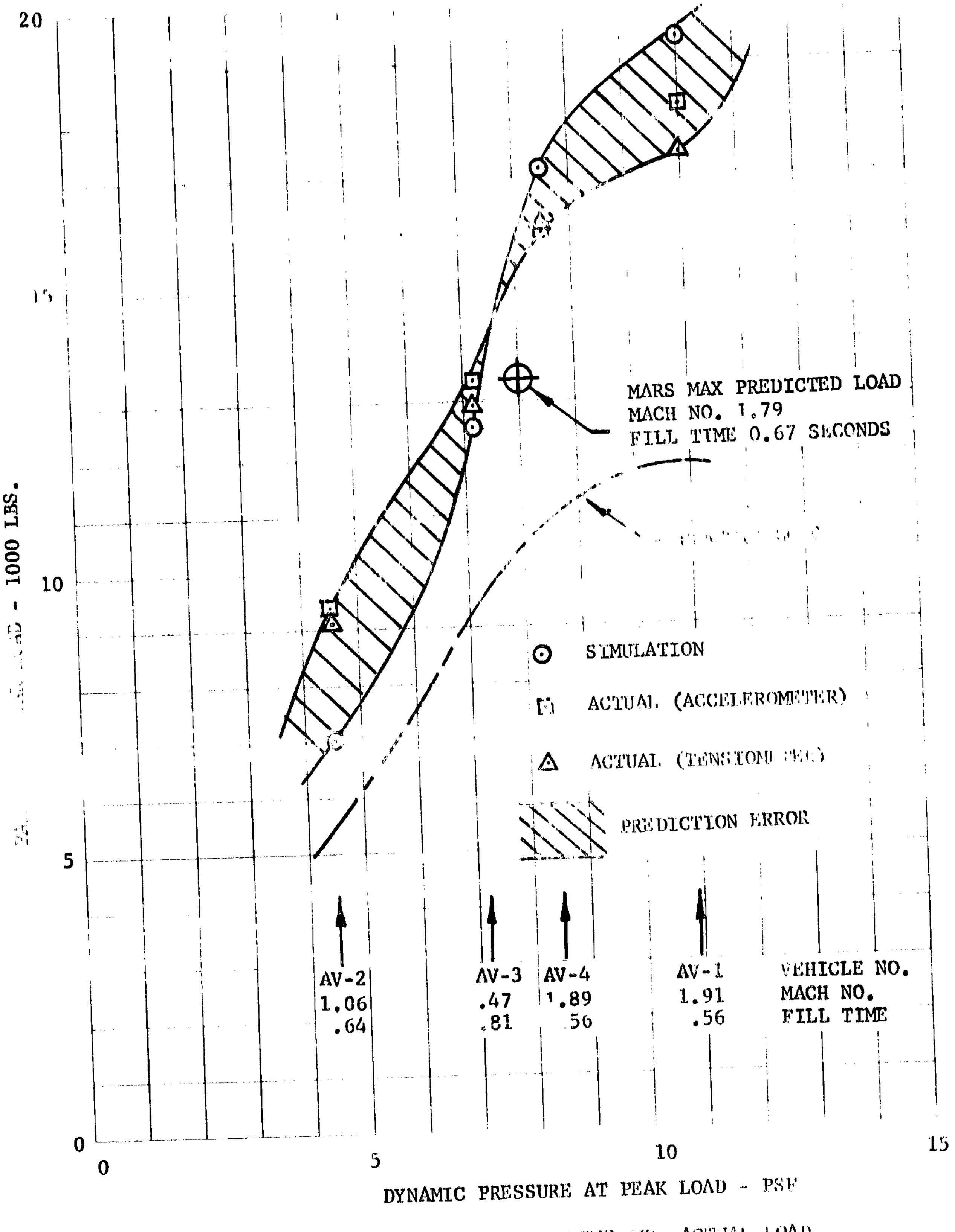

FIGURE 17 PREDICTED VS. ACTUAL LOAD

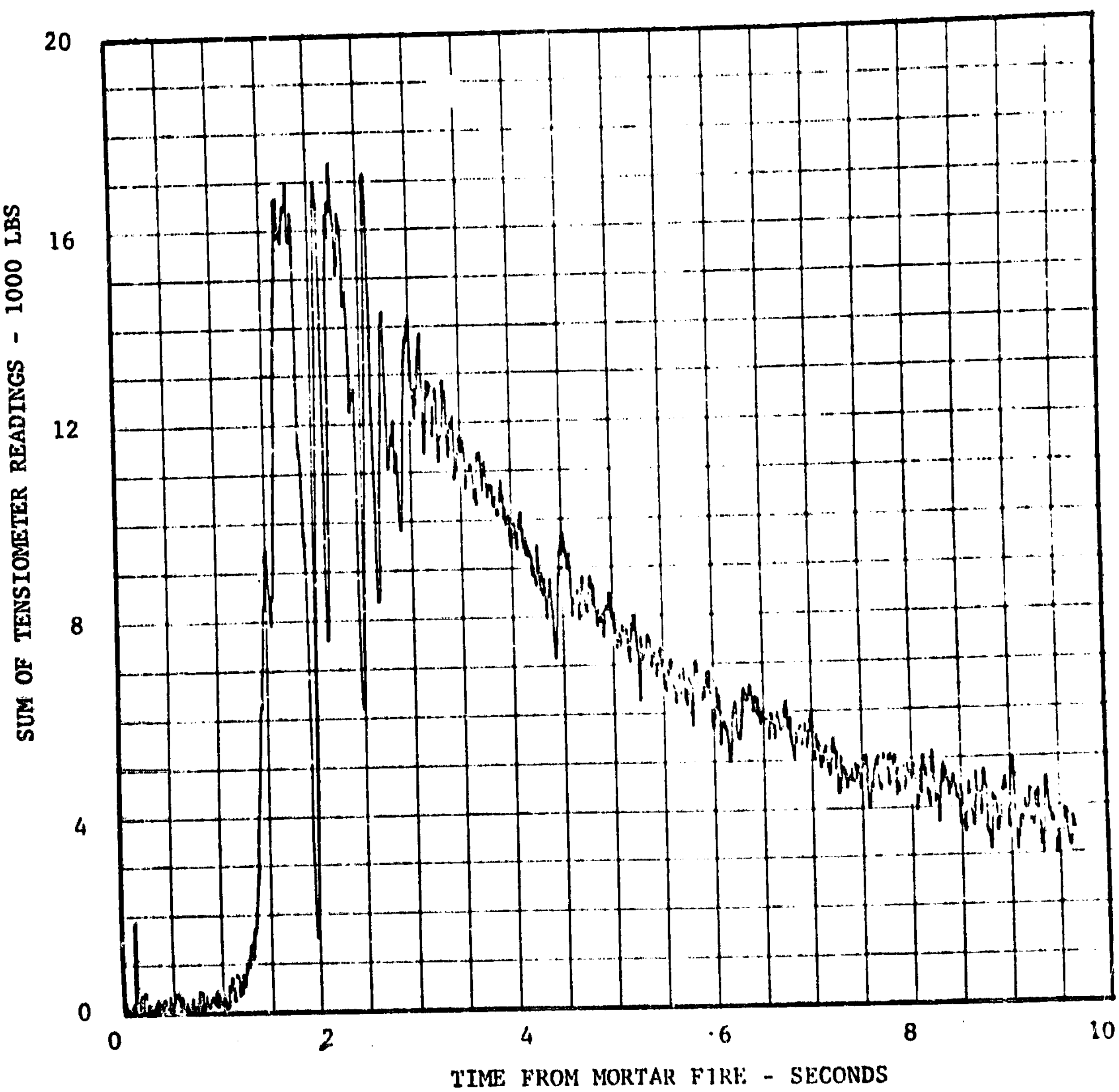

FIGURE 18 PARACHUTE OPENING LOAD, BLDT AV-1

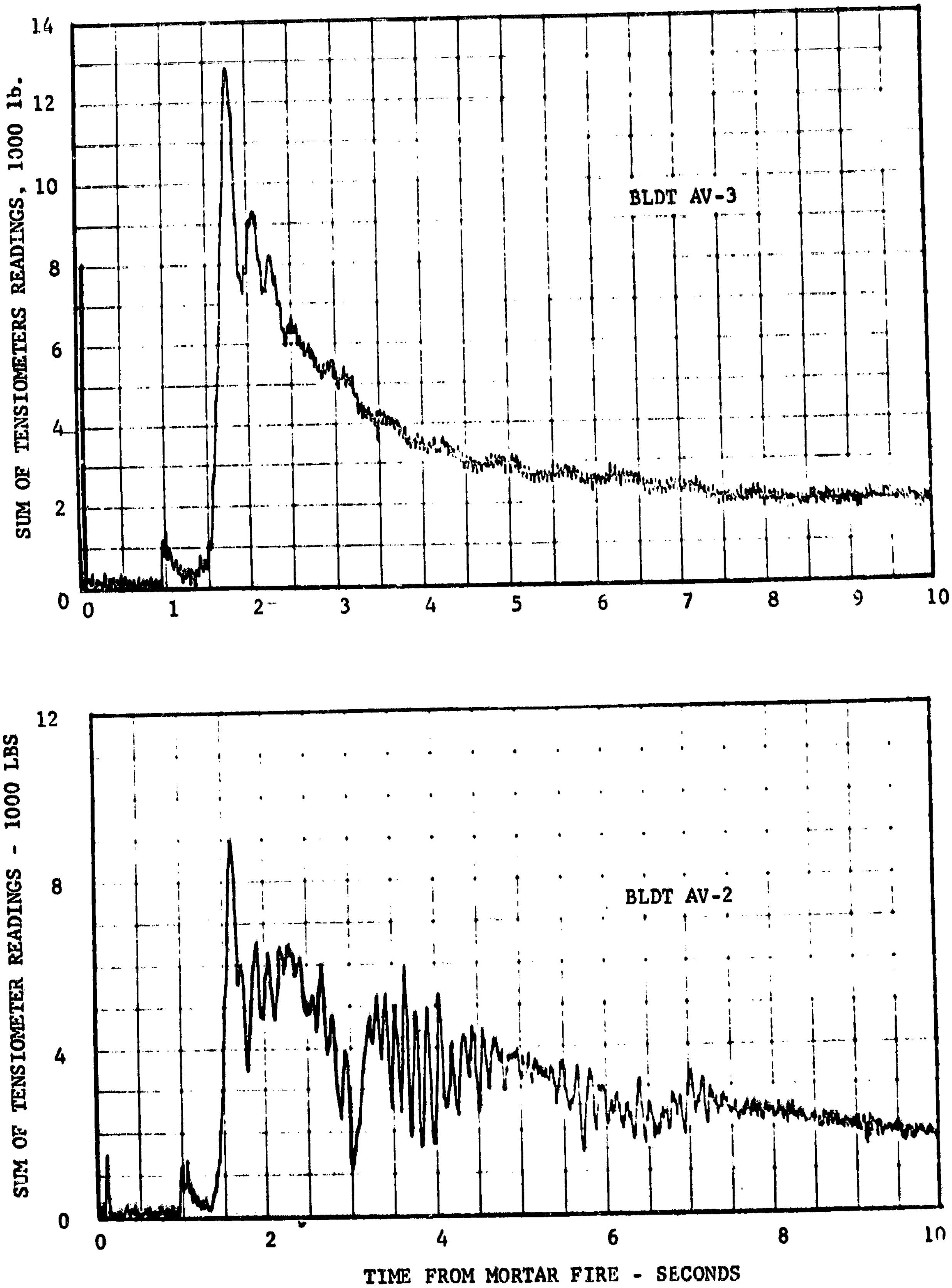

FIGURE 19 PARACHUTE OPENING LOAD, AV-2 AND AV-3

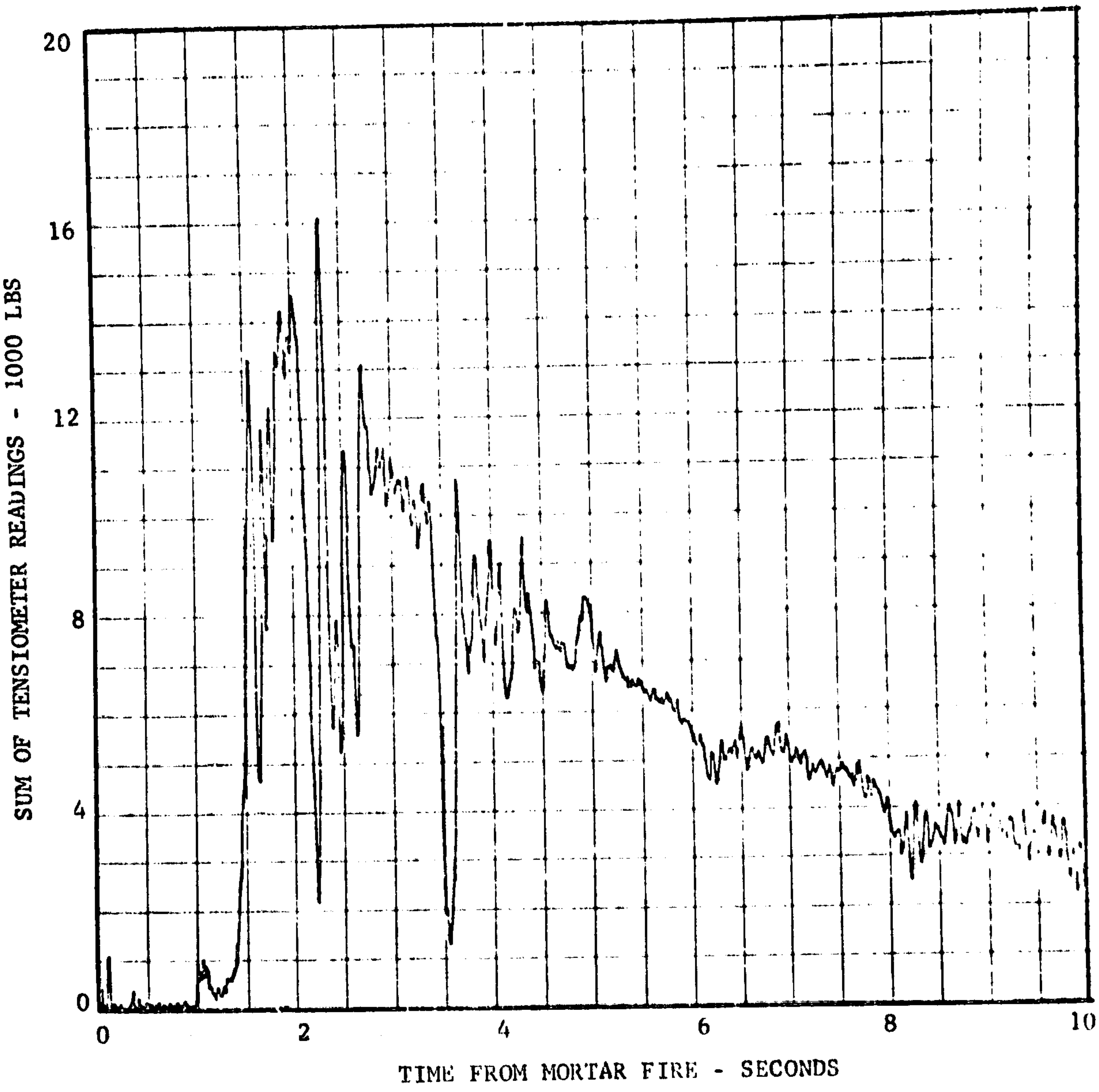

FIGURE 20· PARACHUTE OPENING LOAD, BLDT AV-4

IX. PARACHUTE AND VEHICLE STABILITY

One of the concerns of the decelerator qualification process is the determination of attitudes and attitude rates induced into the lander by the parachute. The following specification from Reference 16 applies to the Mars application:

> "Combined parachute/Viking Lander body response shall be such that lander attitude excursions shall not exceed ±45 degrees from a no-gust trajectory and attitude rates shall not exceed 100 degrees/second with an oscillatory frequency of not less than 1.75 cps at opening shock with requirements decreasing linearly to ±25 degrees and 30 degrees/second by six seconds after mortar fire (4 seconds after parachute full open) and remaining within these latter bounds until terminal engine ignition."

As stated in Section IV, the object of the qualification precedure is to assess these parameters on BLDT and analytically extrapolate them to Mars conditions. The BLDT AV-4 attitude rates from on-board rate gyros in pitch, yaw and roll are shown in Figure 21. At opening shock, the peak attitude rate is 110 degrees/second at a frequency of 2.2 cps. The peculiar beating characteristic in pitch and yaw is simply the projection on the itch and yaw axis of a rolling vehicle of an attitude transient that is initially occurring in a specific plane. The other three BLDT flights had attitude transient response very similar in frequency, damping and general character to that shown for AV-4. Because of the differing load and initial conditions on the other flights, however, the peak attitude rates in degrees/second were 148 (AV-1), 90 (AV-2) and 120.

In order to have confidence in the analytical extrapolation to Mars process, we first must demonstrate confidence in our ability to simulate the BLDT flight results. To achieve good dynamic simulation, the parachute aerodynamic moment coefficient between static trim points had to be reduced to zero and a fictitious pin-connected riser had to be inserted between the bridle and the parachute suspension line apex. Both of these changes allow less constraining influence on the lander by the parachute. The pitch and yaw attitude rates for AV-4 generated by simulation are shown in Figure 22. Very good agreement with the BLDT results in Figure 21 is achieved except at the peak pitch rate point where the error is as high as 35 degrees/second. The differences in peak rates as time progresses gets smaller until the difference practically disappears. The extrapolation process can proceed, however, with this error tolerance in mind.

The BLDT vehicle was aerodynamically similar to the Viking lander, but had different physical properties as indicated in Table 6.

Table 6

PHYSICAL PROPERTY COMPARISON

		BLDT AV-4	Viking Lander
Weight - lbs		1890	1960.6
C. G. offset - Z inches		1.41	1.83
Moment of Inertia - slug-ft^2,	X	437/262	537/333
(Before/after aeroshell	Y	335/227	285/154
separation)	Z	322/214	345/246

Another difference is the fact that the Viking lander has an active attitude control system with 40 ft-lbs torque and capable of controlling the vehicle at deployment to within ± 3 degrees of aerodynamic trim in the presence of wind gusts (Reference 17).

The Mars maximum load case (Mach 1.9 deployment) and the mean deployment have been simulated in detail (Reference 18). The results show the

Viking maximum atti. .de rates to be smaller than the BLDT peak rates largely because of the lower loads, slower filling time, and effect of the attitude control system in controlling deployment conditions and providing rate damping thereafter. A review of the BLDT deployment conditions in Table 2 show that none of the variables in the Table have a good correlation with the variation in peak attitude rates. First peak load, however, shows a strong correlation with the peak rates in Figure 23. The Mars peak rates and loads from simulation are plotted in the same figure and show a consistent trend. By adding an error band of uncertainty associated with our simulation, a peak attitude rate line for Mars extrapolated conditions is generated. If we attach a 1000 lb uncertainty to the maximum predicted Mars opening of 13500 lbs., we observe an extrapolated peak rate of 100 degrees/second which is in agreement with the parachute specification (Reference 16).

The Mars and BLDT simulations both show attitude excursions and rates less than 25 degrees and 30 degrees/second during steady state descent and while experiencing wind gust conditions. BLDT attitude oscillations during descent are shown qualitatively to be within specification in the Figure 24 film sequences taken from the recovery helicopter.

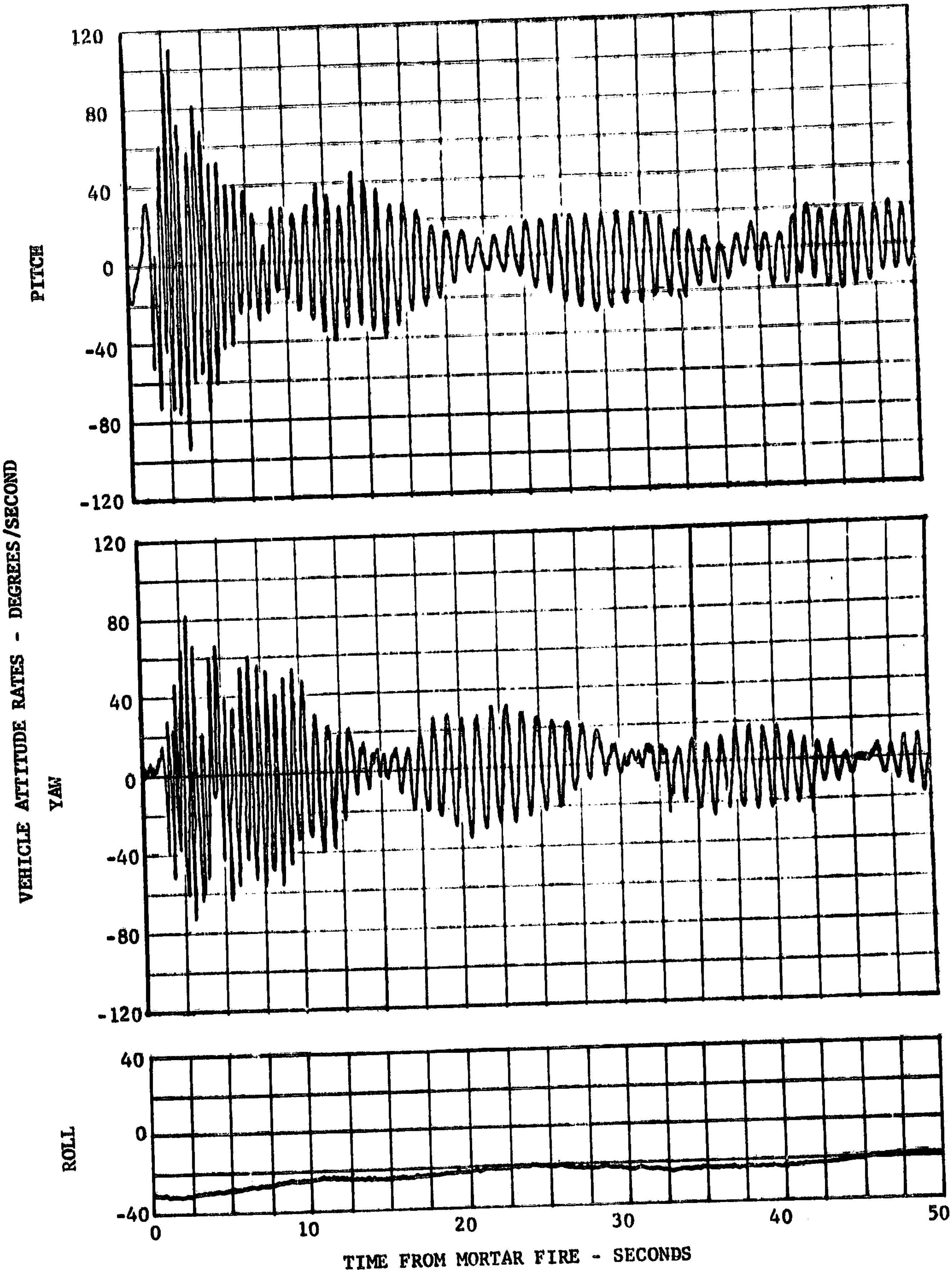

FIGURE 21 VEHICLE ATTITUDE RATES, AV-4 FLIGHT DATA

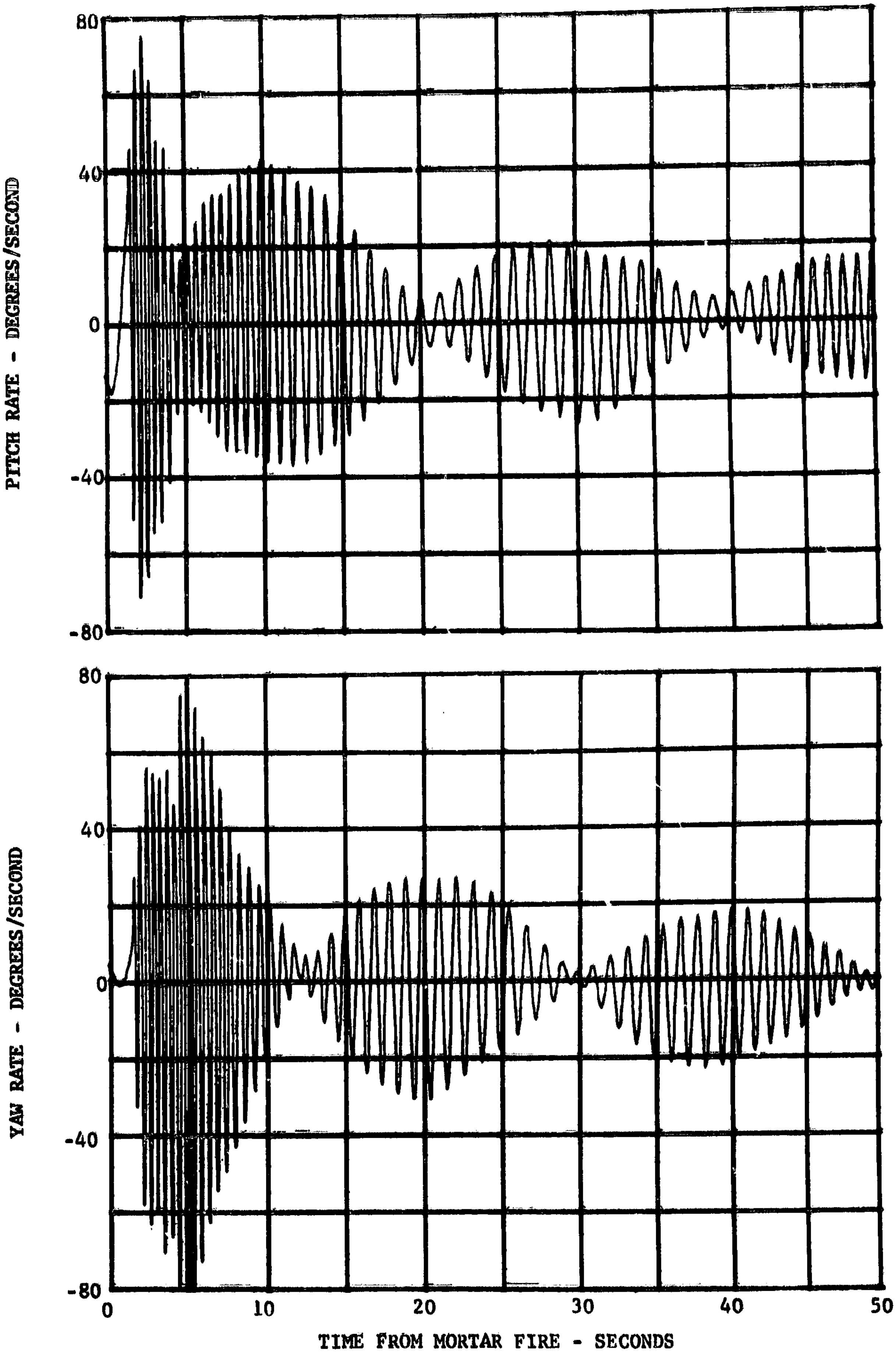

FIGURE 22 VEHICLE ATTITUDE RATES, AV-4 SIMULATION

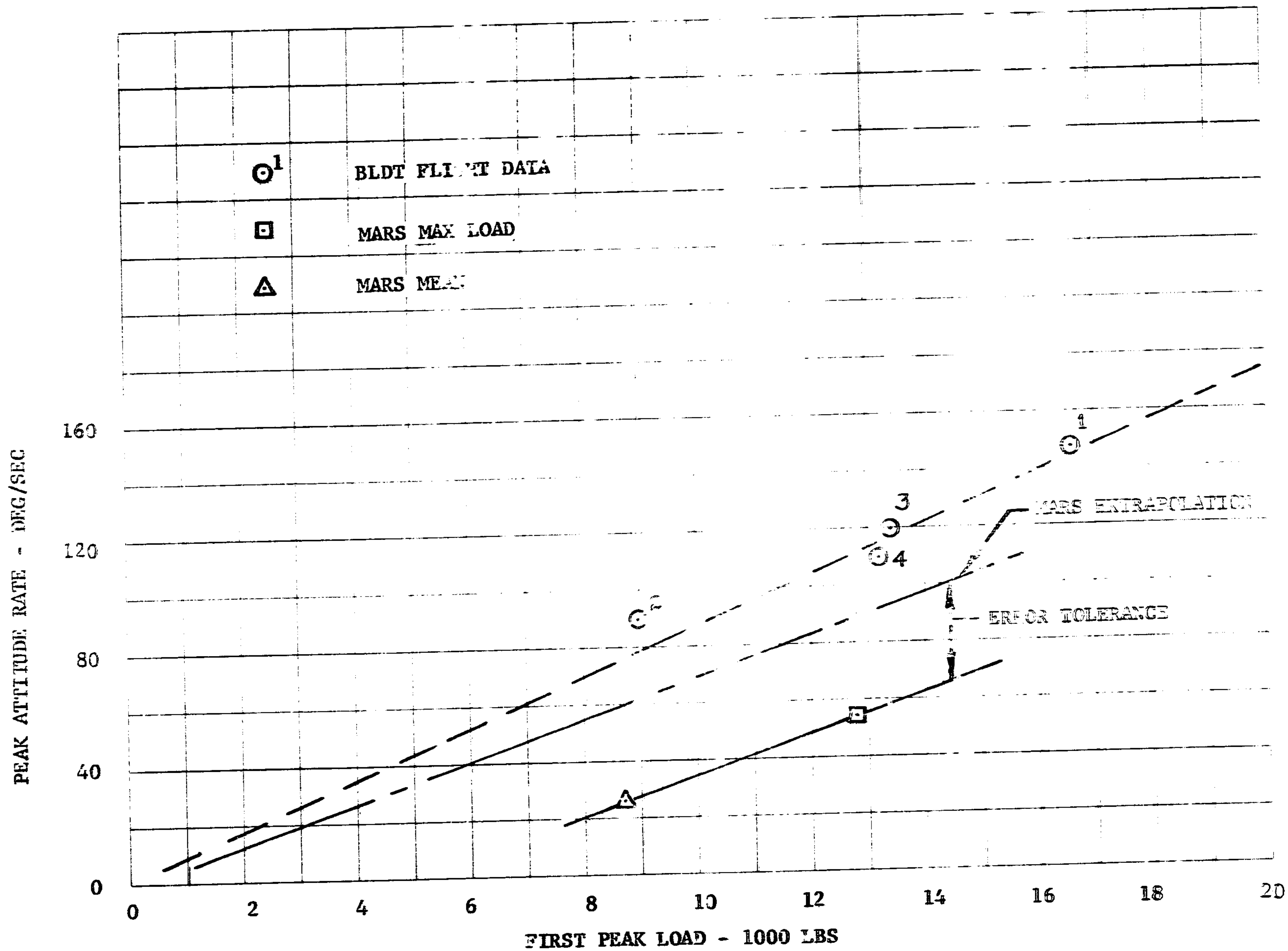

FIGURE 23 ATTITUDE RATE SENSITIVITY TO LOAD

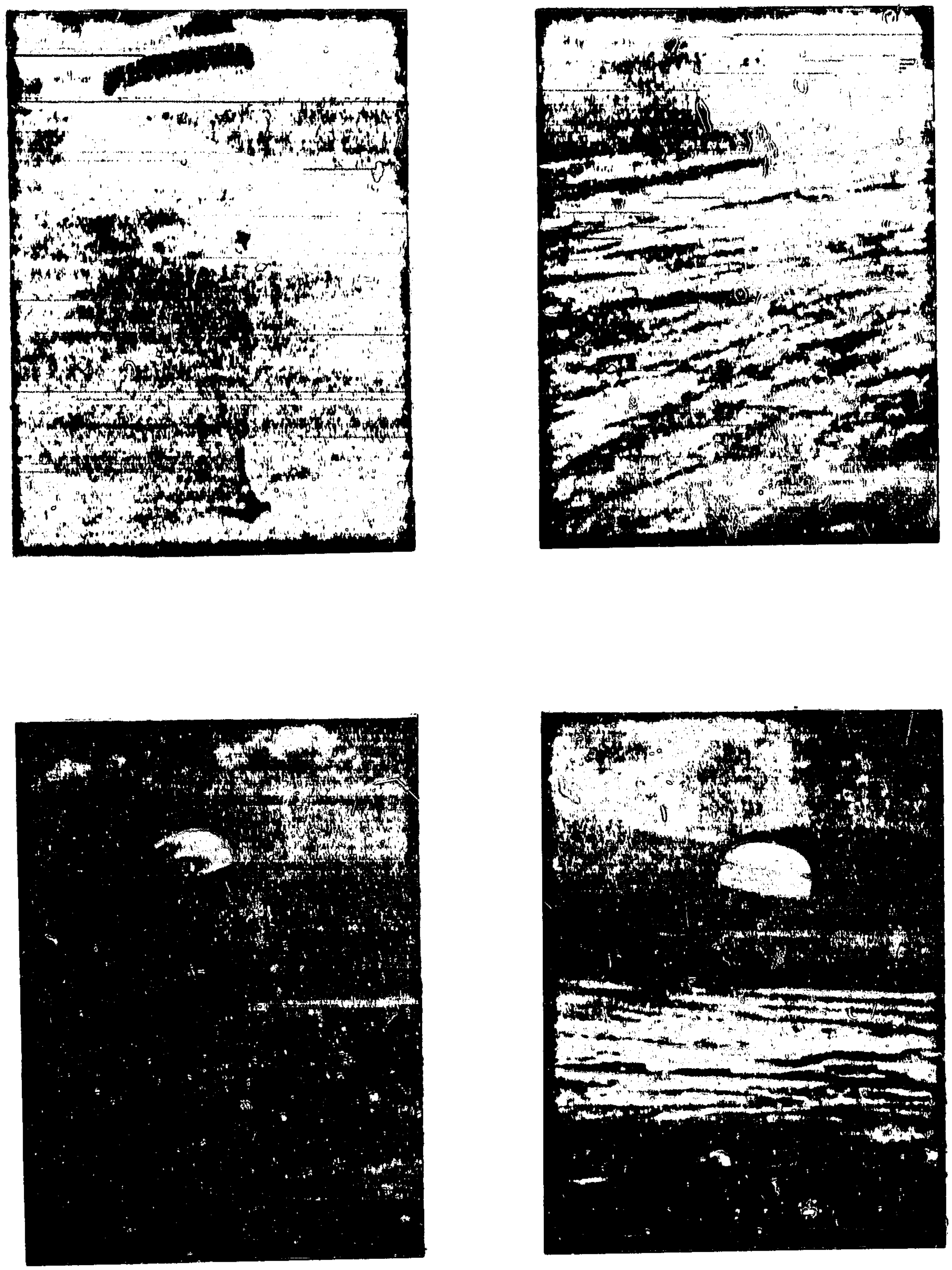

FIGURE 24 SELECTED VIEWS OF PARACHUTE DURING TERMINAL DESCENT

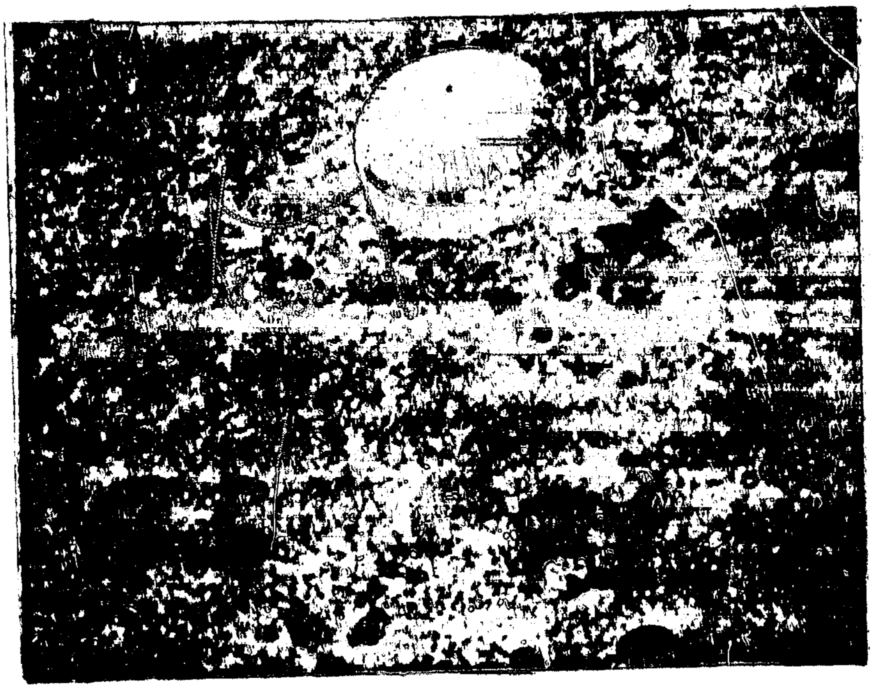

FIGURE 24 SELECTED VIEWS OF PARACHUTE DURING TERMINAL DESCENT (CONTINUED)

X. AEROSHELL SEPARATION

The aeroshell separation system on all BLDT vehicles is similar in design and construction to the system to be used on the Viking lander. The 396 lb. aeroshell is separated 7 seconds after mortar fire in the Viking sequence. On BLDT aeroshell separation is timed to occur when specific Mach number and dynamic pressure conditions occur. Since separation is achieved primarily by virtue of a favorable relative acceleration between bodies, the qualification test conditions should encompass the range of Mach number and dynamic pressure expected on Mars. The BLDT flight conditions at aeroshell separation tabulated in Table 7 are seen to adequately bracket the Mars envelope conditions in Figure 25.

Decelerator qualification is concerned with aeroshell separation primarily from the standpoint of whether parachute drag performance is adequate to meet the qualification requirement of 50 feet of separation in 3 seconds. Observation of the airborne camera film shows no measurable change in the parachute projected area at or shortly after separation. Separation versus time data is obtained from a forward looking Milliken camera which records the aeroshell moving away from the parachute payload. The separation results from all four BLDT flights are seen in Figure 26 to more than adequately meet the qualification requirement. There is little evidence of any parachute drag degradation in the separation data except for a slight change in the slope of the separation curve of AV-1 between 1 and 2 seconds after separation. The Mars envelope shown is predicted by simulation using the nominal predicted parachute drag performance.

Table 7

BLDT AEROSHELL SEPARATION CONDITIONS

	AV-1	AV-2	AV-3	AV-4
Time from Mortar Fire, sec.	9.68	9.1	13.76	7.65
Mach Number	.92	.615	.193	1.18
Dynamic Pressure, psf.	2.42	1.43	1.38	3.18
Time for 1 foot separation, sec.	.15	.18	.21	.16
Time for 50 feet separation, sec.	1.34	1.9	2.05	1.40
Separation Distance in 3 sec.	192	120	97	206

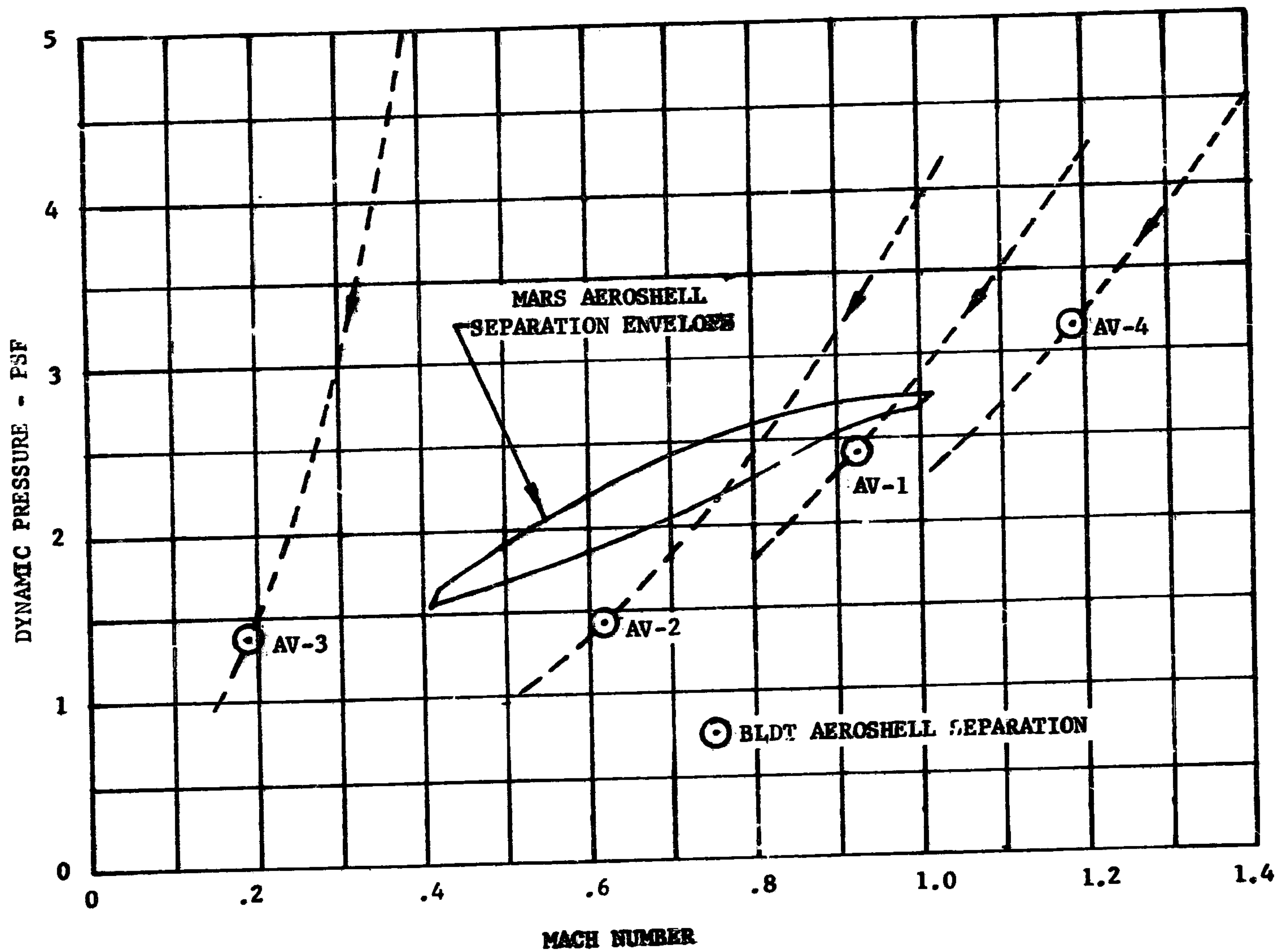

FIGURE 25 AEROSHELL SEPARATION CONDITIONS

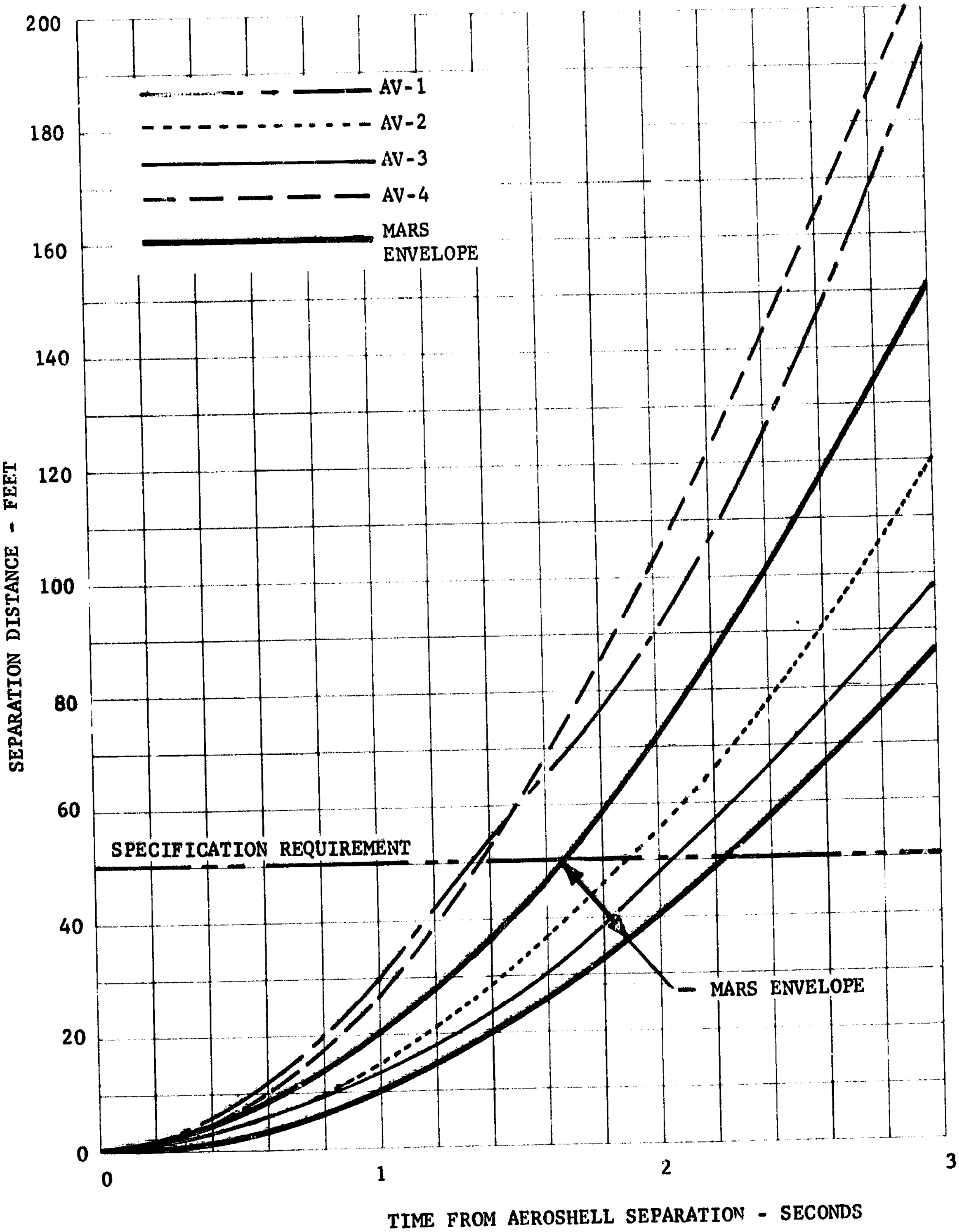

FIGURE 26 AEROSHELL SEPARATION DISTANCE

XI. PARACHUTE STRUCTURAL QUALIFICATION

The Viking decelerator was designed for a design limit load of 17,300 lbs., the pre-BLDT best estimate of maximum Mars opening load. This load readily defines the individual strength requirements for the 48 suspension lines after applying safety and design factors. The determination of canopy materials requires a more sophisticated method of determining stress levels in the disk and band during inflation. In addition, the Viking program must develop enough confidence in the stress prediction capability to allow subsonic development test stress results in the Earth atmosphere to be applied to supersonic qualification flights on BLDT and Mars.

For these reasons, a computerized stress prediction simulation program was developed to predict dynamic stress levels within the parachute as a function of meridian station and time. The basic principle involved equating the work done by the inflation gas during opening of the parachute to the strain energy absorbed by the primary structural components. The work done consists of two additive parts: (1) the differential pressure across the canopy times the change in volume; i.e., $P\Delta V$, and (2) the longitudinal pressure force acting through a distance equal to the stretch in the suspension lines combined with the change in canopy height during inflation.

A series of subsonic drop tests were first carried out with the full scale system at altitudes of about 50,000 feet. In these tests careful attention was given to establishing dynamically similar environments, insofar as possible, to those postulated for operation on Mars. Design conditions for these tests were also established by taking into account possible differences in subsonic and supersonic effective drag coefficient. Thus these tests were a practical means of approaching near Mars ultimate stress conditions in a cost-effective manner.

A predicted stress plot for the Viking structural design case is presented in Figure 27. As indicated, working stress (i.e., with no design or safety factor) is presented both as a function of non-dimension inflation time, y, and meridian location. The plots are characterized by high stresses in the disk cloth near the vent during early inflation. As time increases, however, the outboard locations increase in load. A peak working stress of about 42 lb/in. is achieved in the disk and 22 lb/in. in the band. Disk and band material strengths are 115 and 72 lb/in respectively. Similar subsonic drop test predictions have been made. Typically, a relatively higher loading is produced in the crown area of the canopy for limit load tests owing to the comparatively slower inflation. For over-load tests, however, a comparatively higher indicated stress was produced in the band. Comparative results are shown in the table below.

Table 8

Comparative Subsonic Test Data and Stress Predictions

Subsonic Test No.	Peak Load (lbs)	Peak Load (% of Viking)	Disk Stress (% of Viking)	Band Stress (% of Viking)
LADT 1	17,650	100	98	88
LADT 2	9,300	53	94	88
LADT 3	26,318	149	157	162
LADT 4	24,225	137	131	157
LADT 5	23,900	135	129	154
LADT 6	18,600	105	103	93
LAQT 2	22,200	126	121	136
LAQT 3	23,200	131	126	146

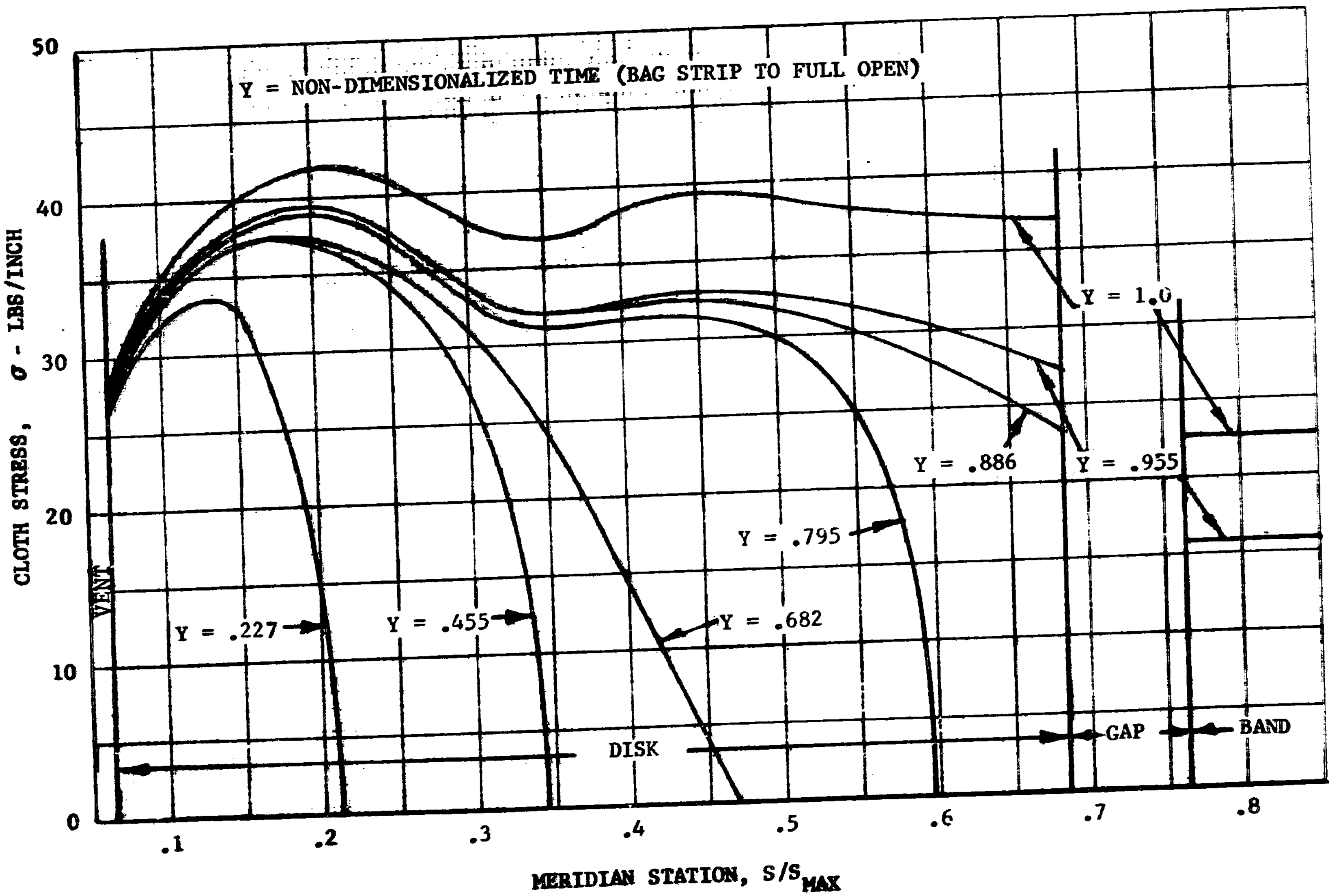

FIGURE 27 PARACHUTE CLOTH STRESS DURING INFLATION

XII. PARACHUTE RECOVERY SUMMARY

The parachute was successfully recovered on each of the BLDT flights. Detailed post flight inspection data is included in References 2 through 5. The only significant damage occurred on AV-1 at an overtest load condition. The AV-1 prachute canopy sustained radial tears from the vent to the edge of the disk in gores 36 and 38 early in the inflation cycle. Analysis of the nature of the tears and the fact that they occurred much prior to peak canopy load leads to the conclusion that the failed panels sustained frictional damage as they emerged from the deployment bag. The excessive dynamic pressure reduced the bag stripping velocity, allowing a significant amount of canopy inflation prior to bag strip. This behavior is felt to have caused the bag stripping damage. These areas were then exposed to localized high pressure during an unsymmetrical canopy inflation which caused the small initial damage to propagate into large tears. In spite of the damage sustained to the canopy, the parachute maintained structural integrity and produced sufficient drag for a successful Mars mission.

On the powered flights, a few small holes and black smudge marks were attributed to hot rocket exhaust particle impingement on the canopy. Particles can be seen in the airborne camera film proceeding aft from the vehicle during rocket motor tail-off prior to and during the deployment process. There was evidence that a few minor cuts may have resulted from friction burns along fold lines during bag strip.

Complete pre-flight and post-flight measurements (References 2-5) show interesting permanent deformations in structural components. The suspension lines show the most significant permanent set which is of interest to the opening load simulation model. Between pre-flight measurement and post-flight measurement, the parachute undergoes a heat sterilization cycle which tests have shown causes a 2 percent shrinkage in suspension lines. After allowing for this effect, the test results show an average 7 foot suspension line length increase on the maximum load case (AV-1), a 3 foot average length increase on the next highest load case (AV-4) and little, if any, permanent set on the lower load cases (AV-2 and AV-3). The implication of this data is that the deformation up to some load level may be almost entirely elastic. This information may help improve our opening load prediction technique.

XIII. PARACHUTE DRAG PERFORMANCE

The parachute incremental drag evaluation is based on the definition of a drag coefficient:

$$C_{D_P} = \frac{2ma}{\rho V^2 S} - \frac{C_{D_F} \cdot S_F}{S}$$

where: m = Vehicle mass, slug

a = Acceleration, fps

ρ = Freestream density

V = Vehicle relative velocity, fps

S = Reference area, 2206 ft^2

$C_{D_F}\ S_F$ = Forebody drag area, ft^2

The vehicle mass was given in the BLDT vehicle performance reports, References 2 to 5, as was atmospheric data and forebody drag coefficient. The vehicle acceleration, although measured with on-board instrumentation, was obtained primarily from radar, since the inertial attitude of the vehicle was not reconstructed during descent. The radar tracking data was differentiated twice to give position, velocity and acceleration using a least squares filter over various time intervals depending on the noise level in the radar data. The relative velocity vector was obtained by subtracting the wind components whereas the aerodynamic acceleration vector was obtained by adding gravity to the inertial accelerations. The component of this aerodynamic acceleration vector along the velocity vector was caused by drag and the normal component is lift. During the early deployment stages where the acceleration was varying, the accelerometer data was used to obtain the drag. The composite drag coefficient curves for the flights are shown in Figure 28.

The lift coefficient which was obtained is shown in Figure 29. The lift does not appear to be significant until subsonic speeds are reached. The AV-1 parachute did not produce as much lift as the other three parachutes probably due to the damage which occurred during deployment. The lift which was produced by the parachutes shows up quite clearly in the trajectory during the vertical descent. Figures 30 thru 33 show how the horizontal velocity components of the trajectory oscillate about the wind. This relative velocity is caused by a lift acceleration which is rotating about the velocity vector. The phasing between the directions indicate a somewhat constant lift vector which is moving in a circular pattern rather than a swinging from side to side. This shows up when the horizontal relative velocity components are plotted against each other as in Figures 34 and 34. The direction of this lift vector is also presented in Figure 36. The evaluation of the lift is strongly dependent on the accuracy of the winds data especially at low altitudes where the descent velocity is low. Small errors in the winds data is reflected in the evaluation of both dynamie pressure and the lift vector. Due to this uncertainty in the magnitude of this lift, this portion of the trajectory was analyzed by assuming zero lift, and the descent rate was converted to a dynamic pressure. This terminal dynamic pressure is shown in Figure 37 for the four flights together with the altitude and Mach number. The data shows a reduction in dynamic pressure below approximately 40,000 ft. ($M \leq 0.05$) which is indicative of a rise in the incremental parachute drag coefficient, which is also shown. This drag variation is compared to the low altitude bomb drop tests (LADT) in Figure 38. These low altitude tests included ballast which was dropped at approximately 20,000 ft. Prior to ballast dump, the total vehicle weight was higher than the BLDT weight ($\approx$ 2600 lbs) and after ballast dump it was lower ($\approx$ 600 lbs). A similar drag rise below $M \approx 0.05$ was indicated during these tests. Since this drag change occurs in the troposphere, it has been speculated that the deviation in drag coefficient from the nominal could be caused by a parachute cloth elongation with temperature under load. This would explain the higher supersonic drag since the cloth temperature would be high due to aerodynamic heating. Although the unstressed length of Dacron fibers tend to shrink at higher temperatures, this trend can be easily reversed by the increase in resiliancy with temperature. This drag rise occurs at a Reynolds number $\approx 5 \times 10^6$ based on D_o, however there is no known reason why the drag should increase either below such a Mach number, nor above this Reynolds number. The Mars flight conditions will be above this Mach number, below this Reynolds number and at colder temperatures which diminishes the importance of this drag rise.

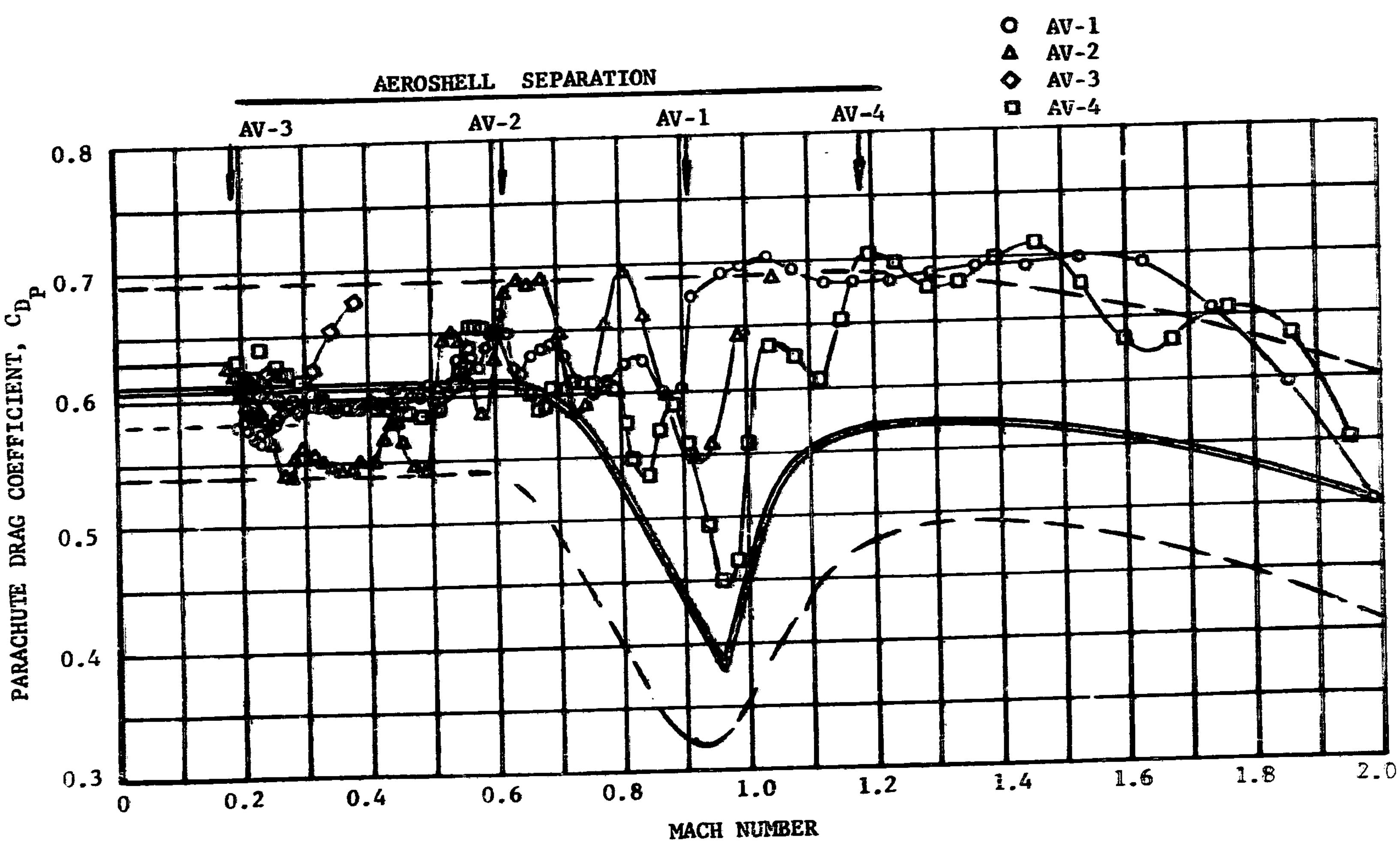

FIGURE 28 PARACHUTE DRAG COEFFICIENT

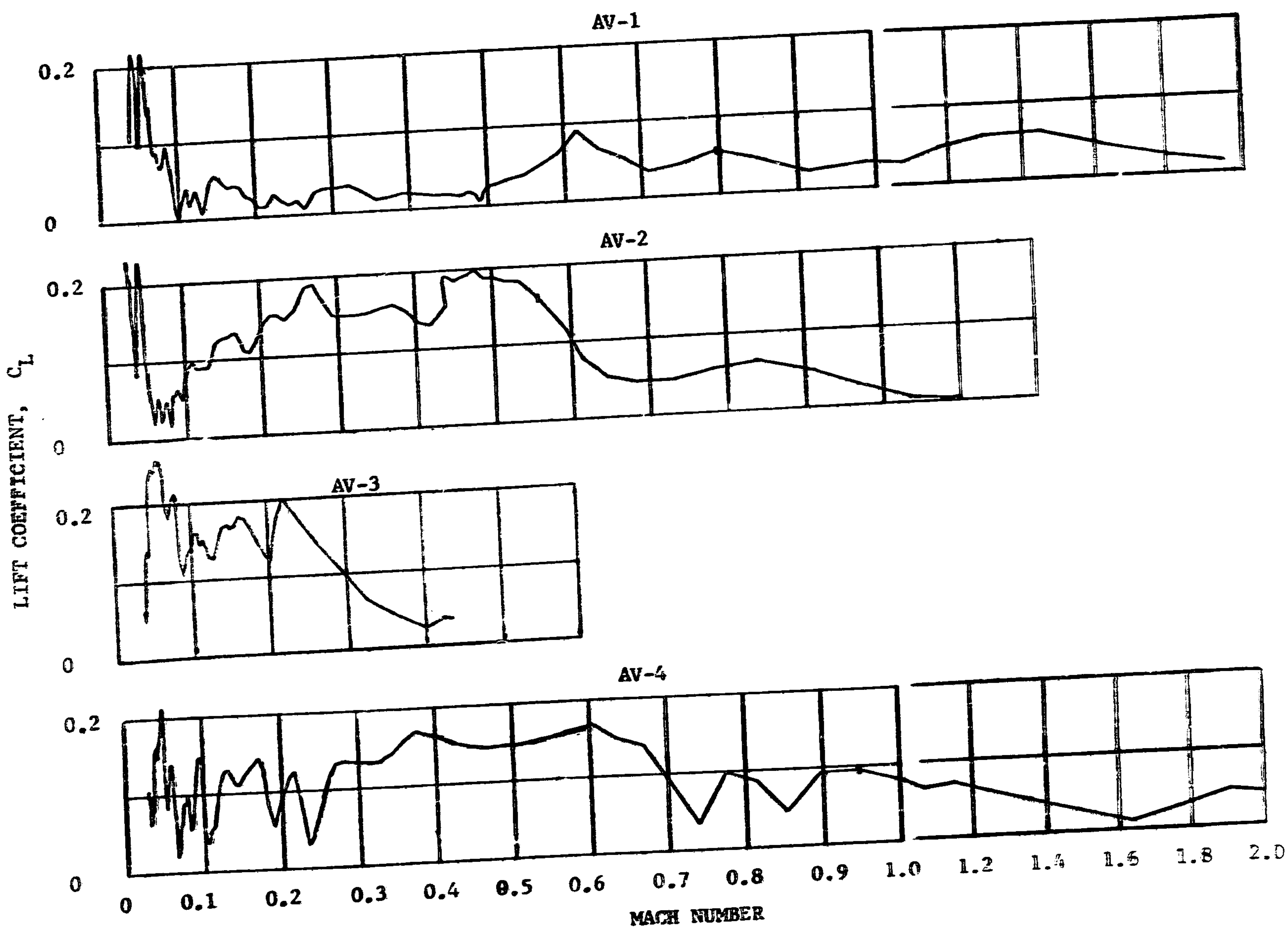

FIGURE 29 PARACHUTE LIFT

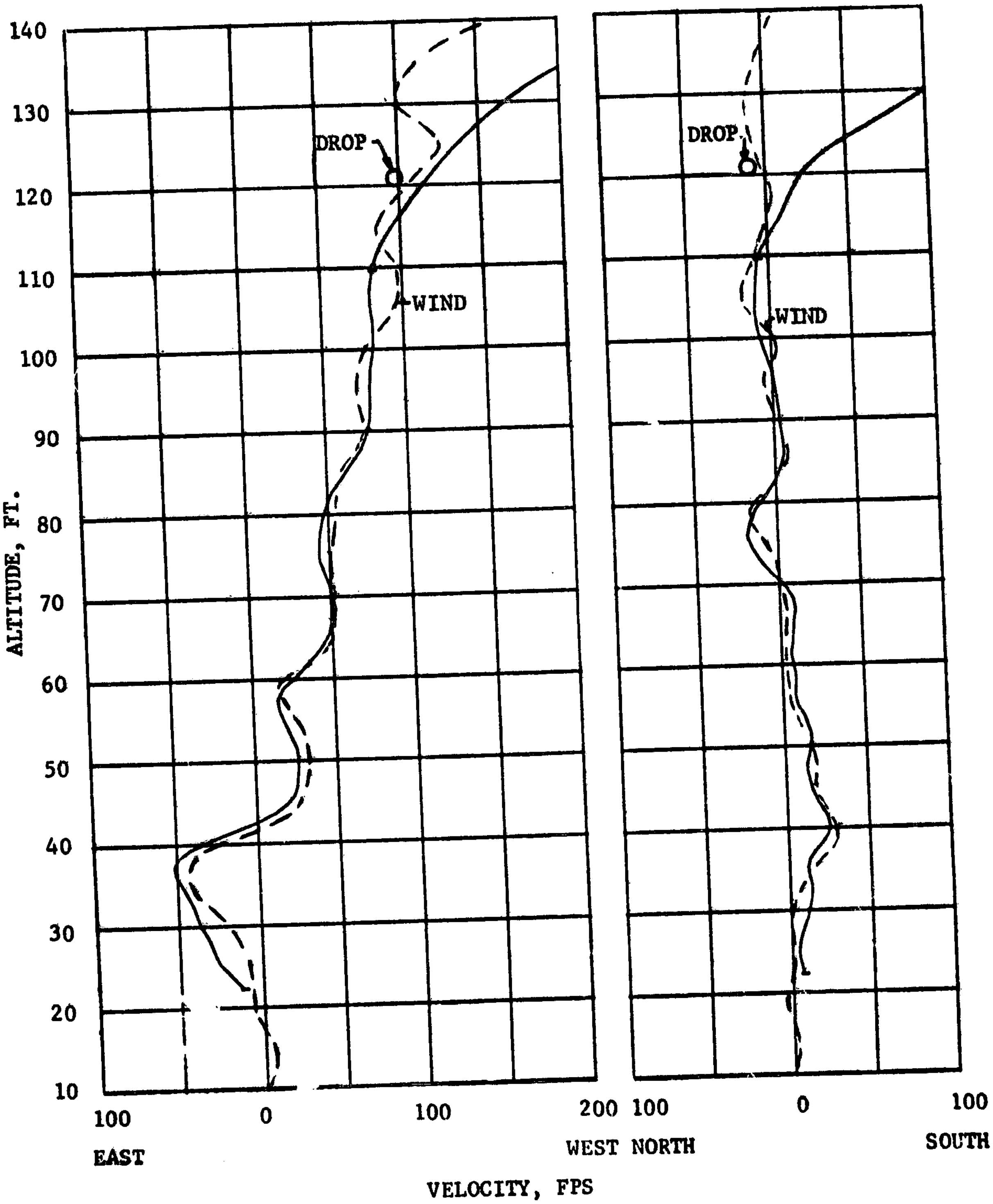

FIGURE 30 HORIZONTAL VELOCITY COMPONENTS, AV-1

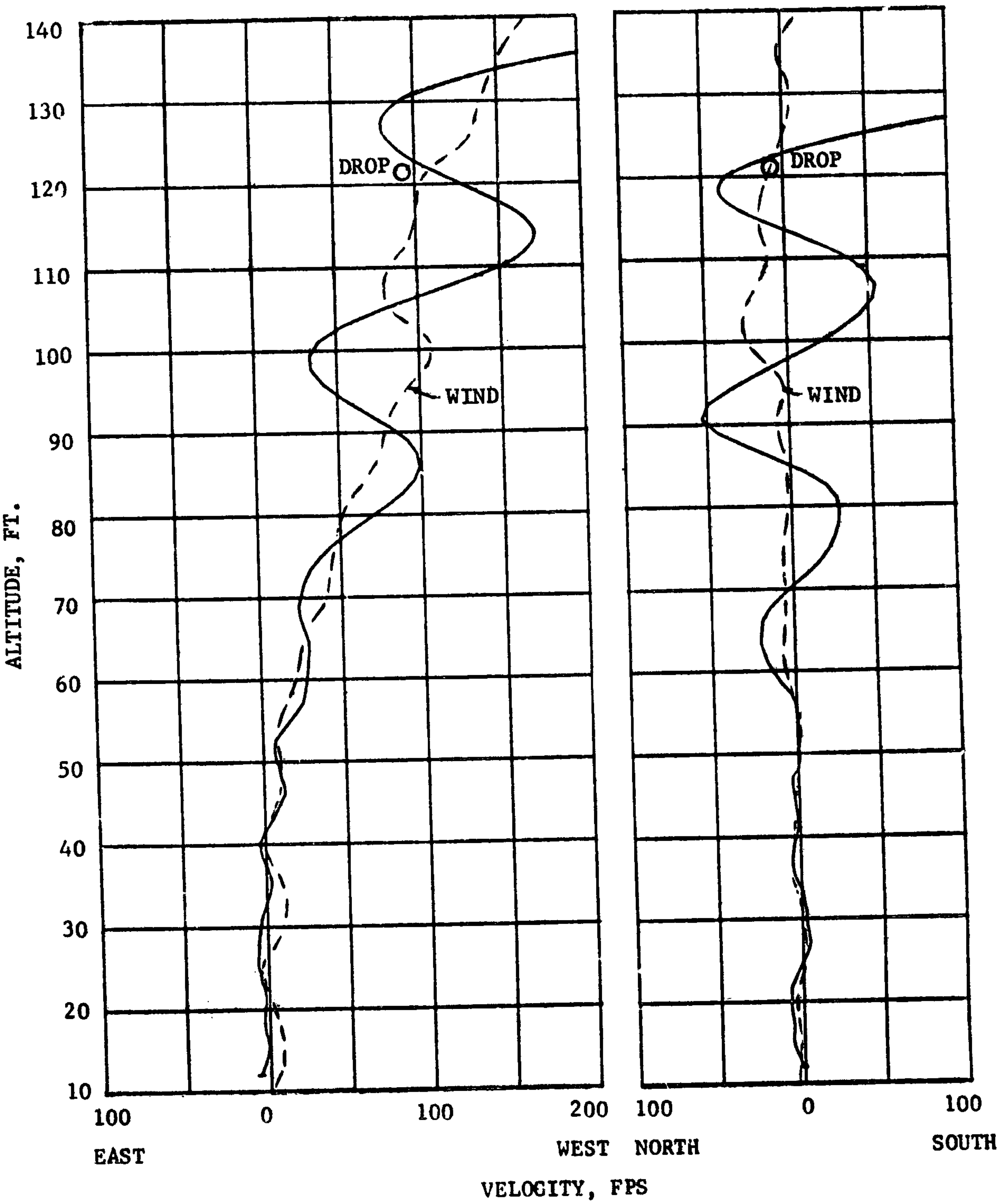

FIGURE 31 HORIZONTAL VELOCITY COMPONENTS, AV-2

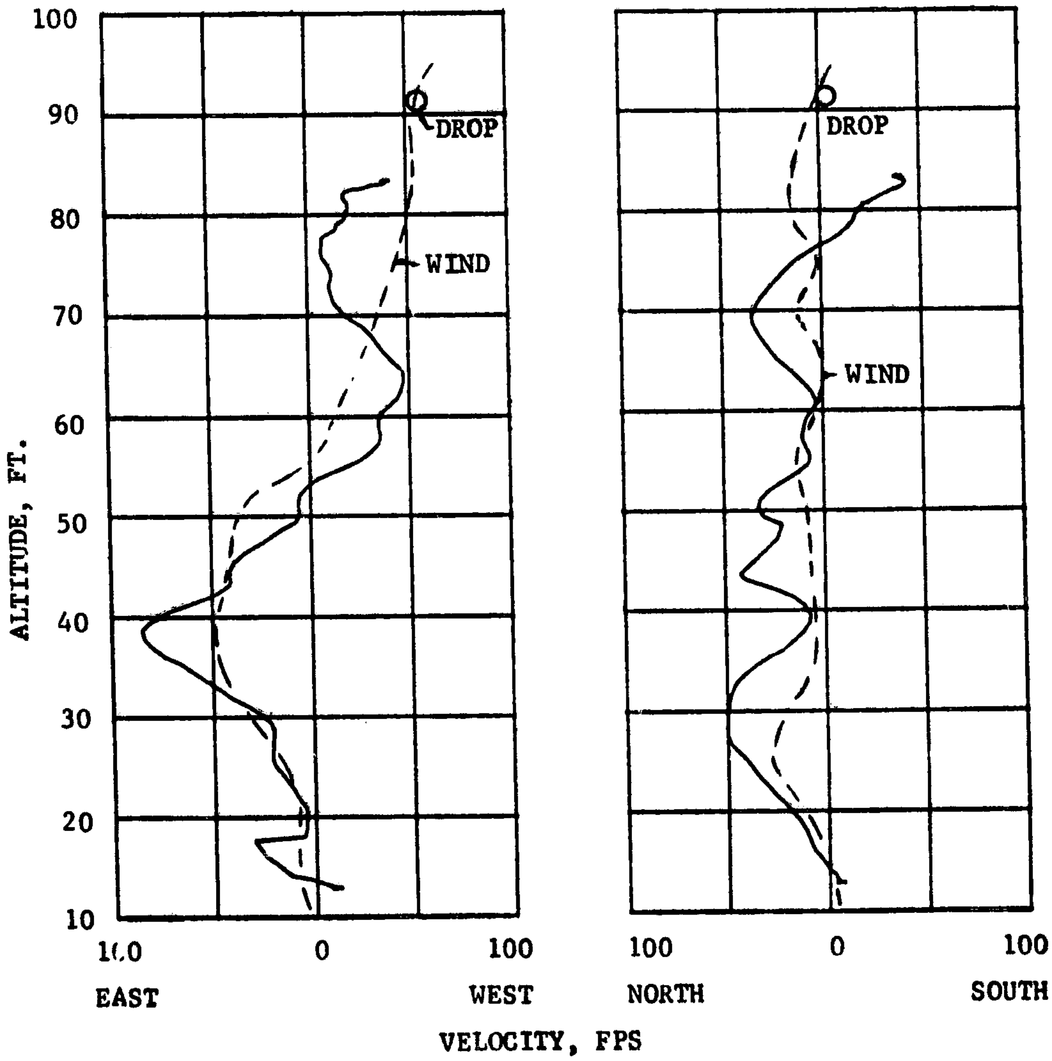

FIGURE 32 HORIZONTAL VELOCITY COMPONENTS, AV-3

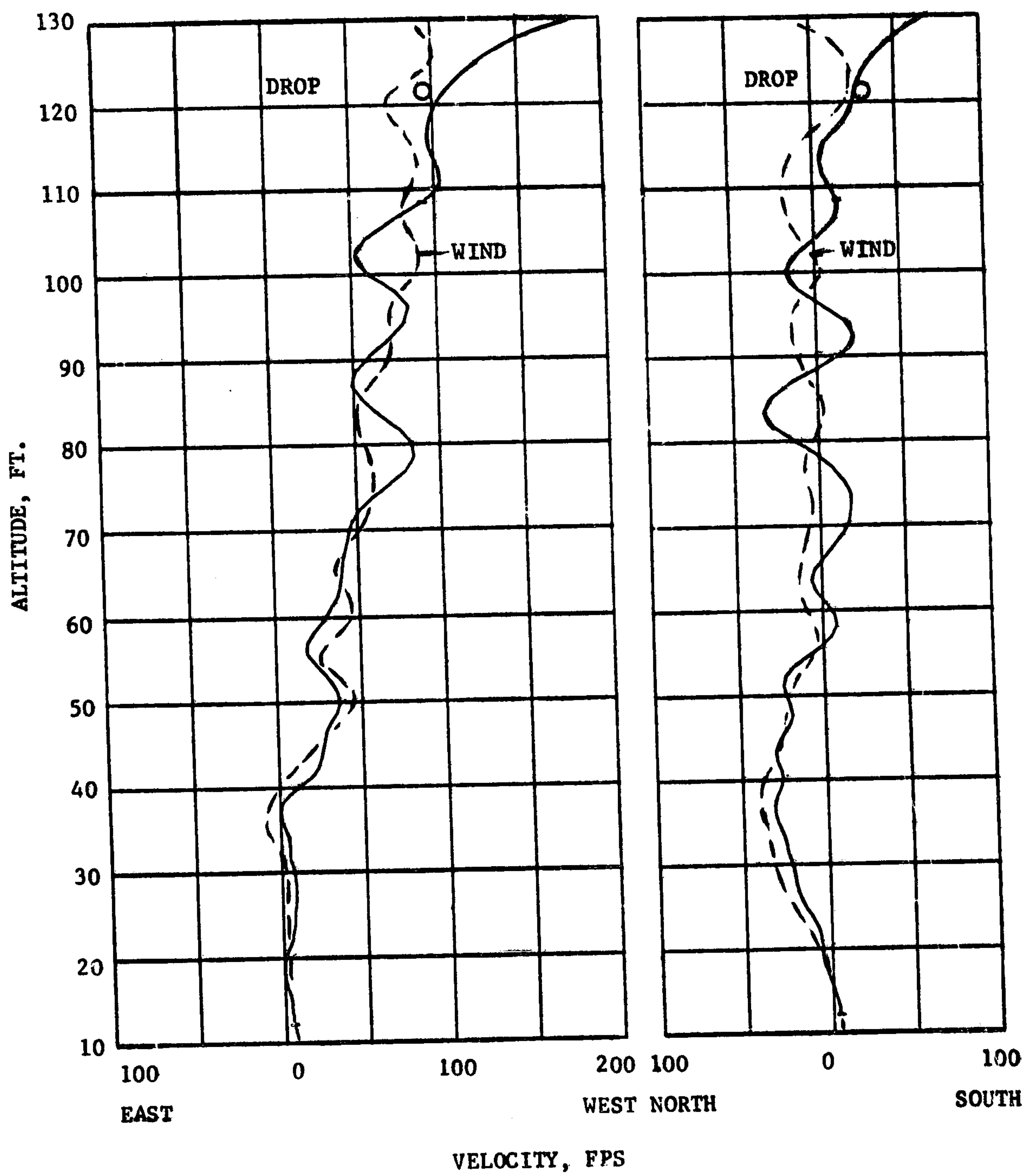

FIGURE 33 HORIZONTAL VELOCITY COMPONENTS, AV-4

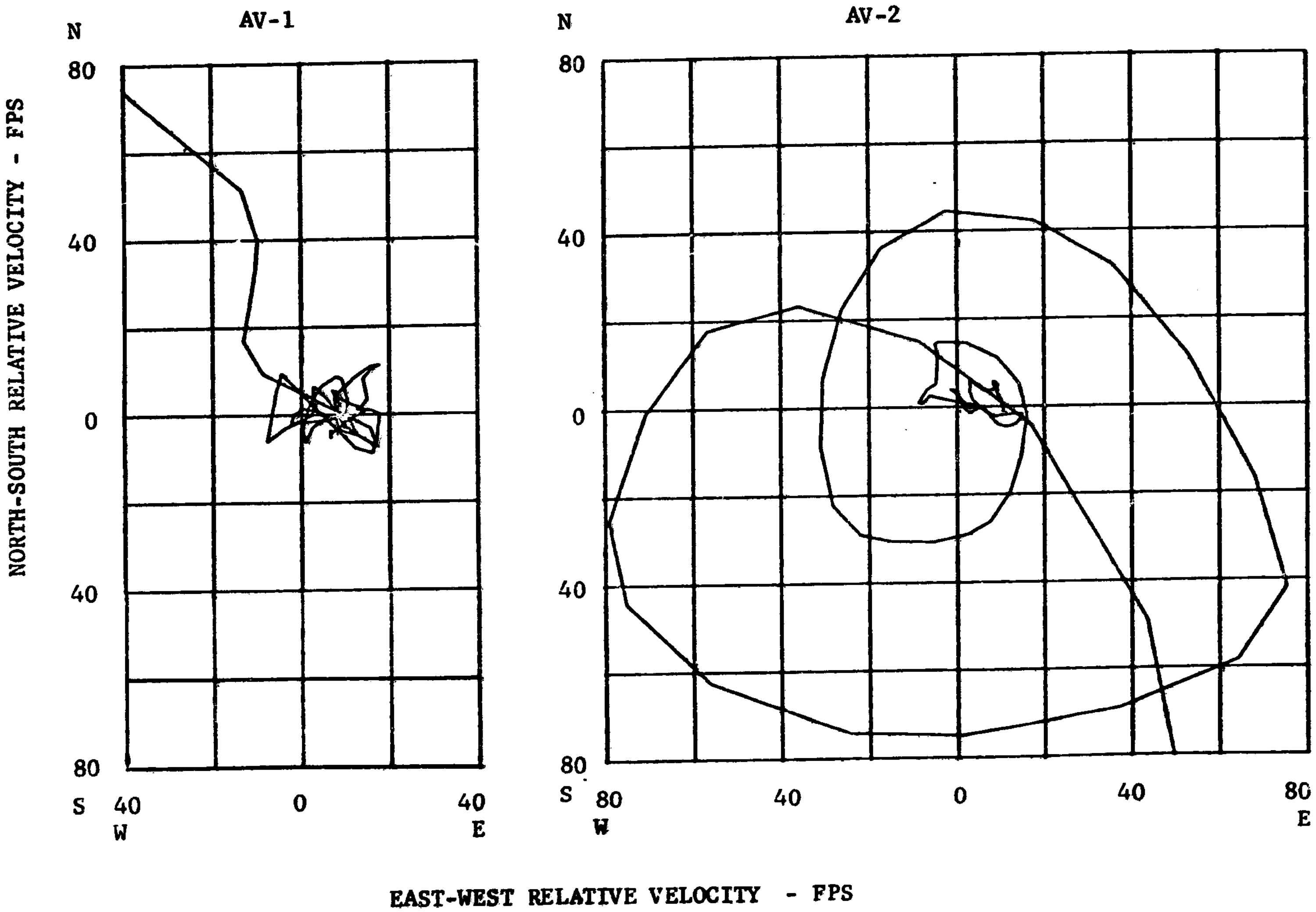

FIGURE 34 RELATIVE VELOCITY PHASE PLANE, AV-1 and AV-2

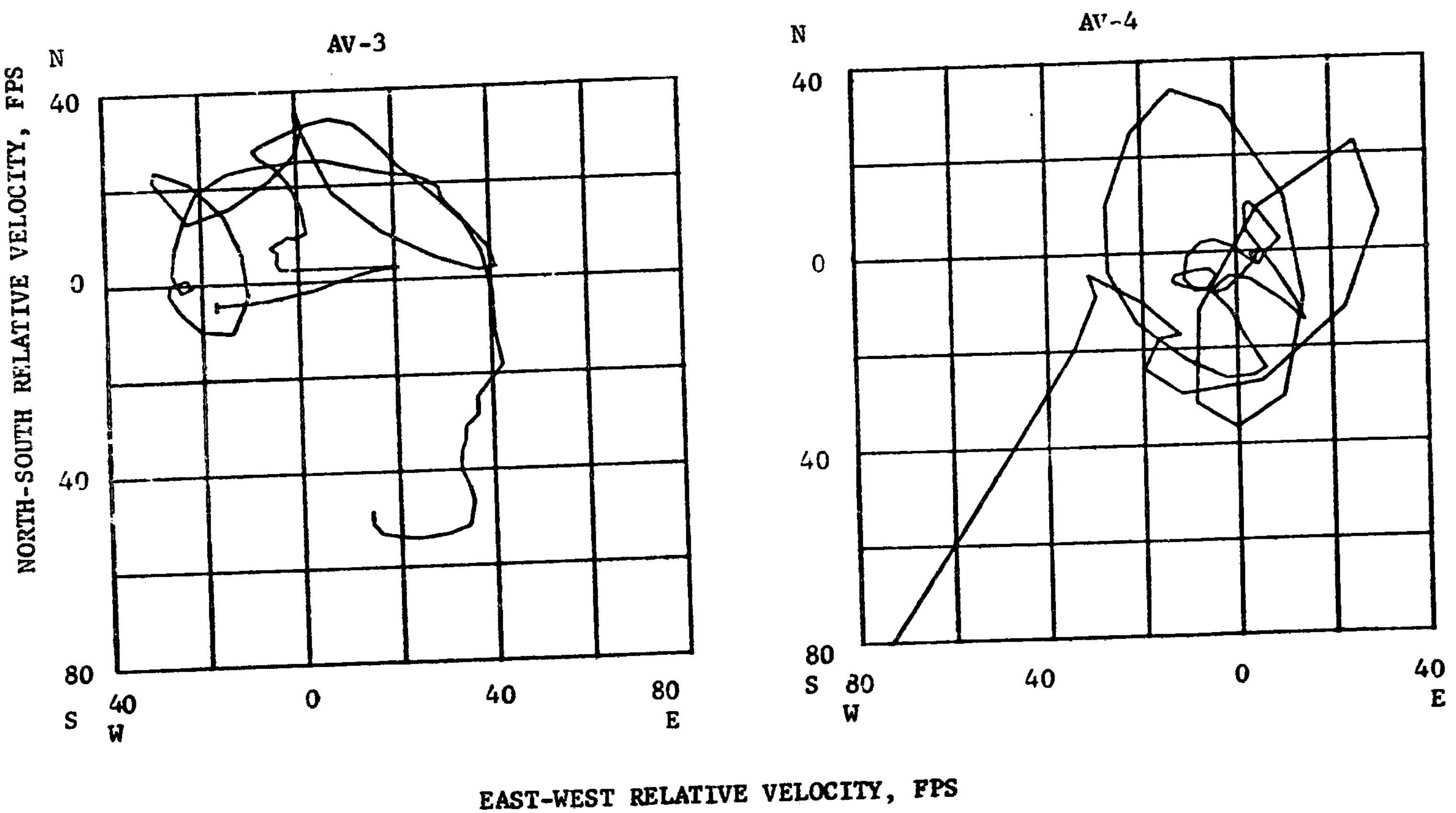

FIGURE 35 RELATIVE VELOCITY PHASE PLANE, AV-3 AND AV-4

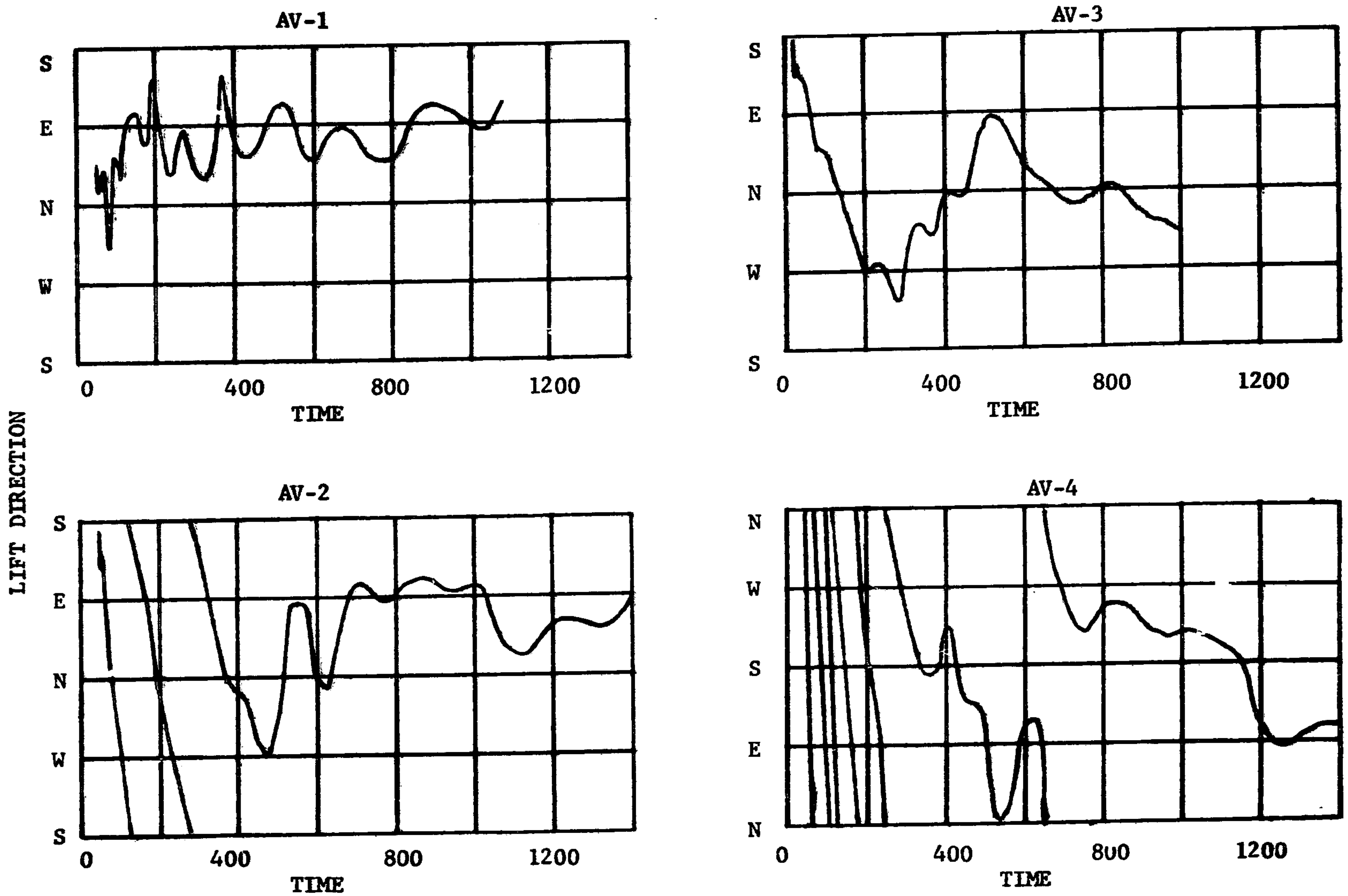

FIGURE 36 LIFT VECTOR DIRECTION

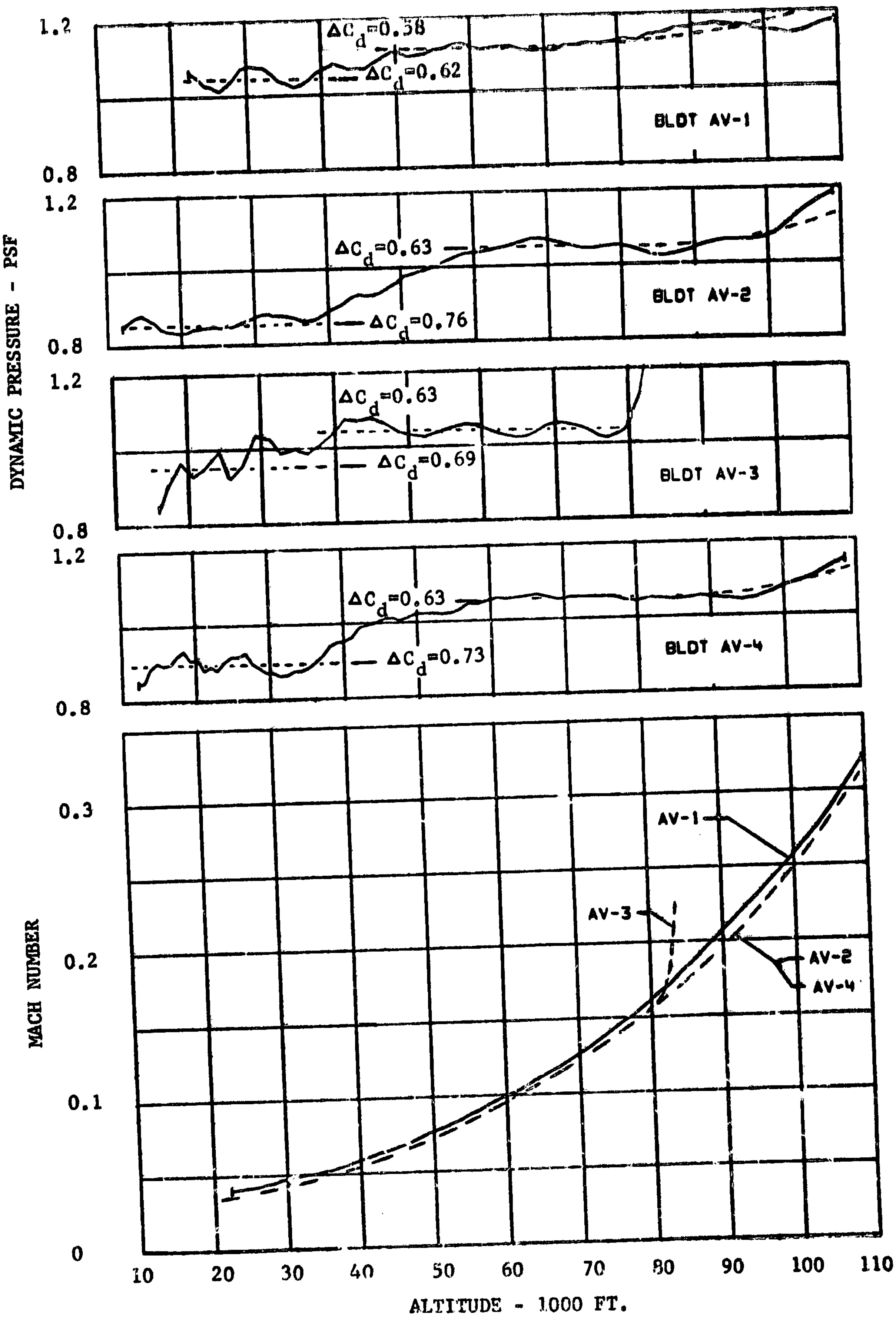

FIGURE 37 PARACHUTE ZERO LIFT TERMINAL DYNAMIC PRESSURE

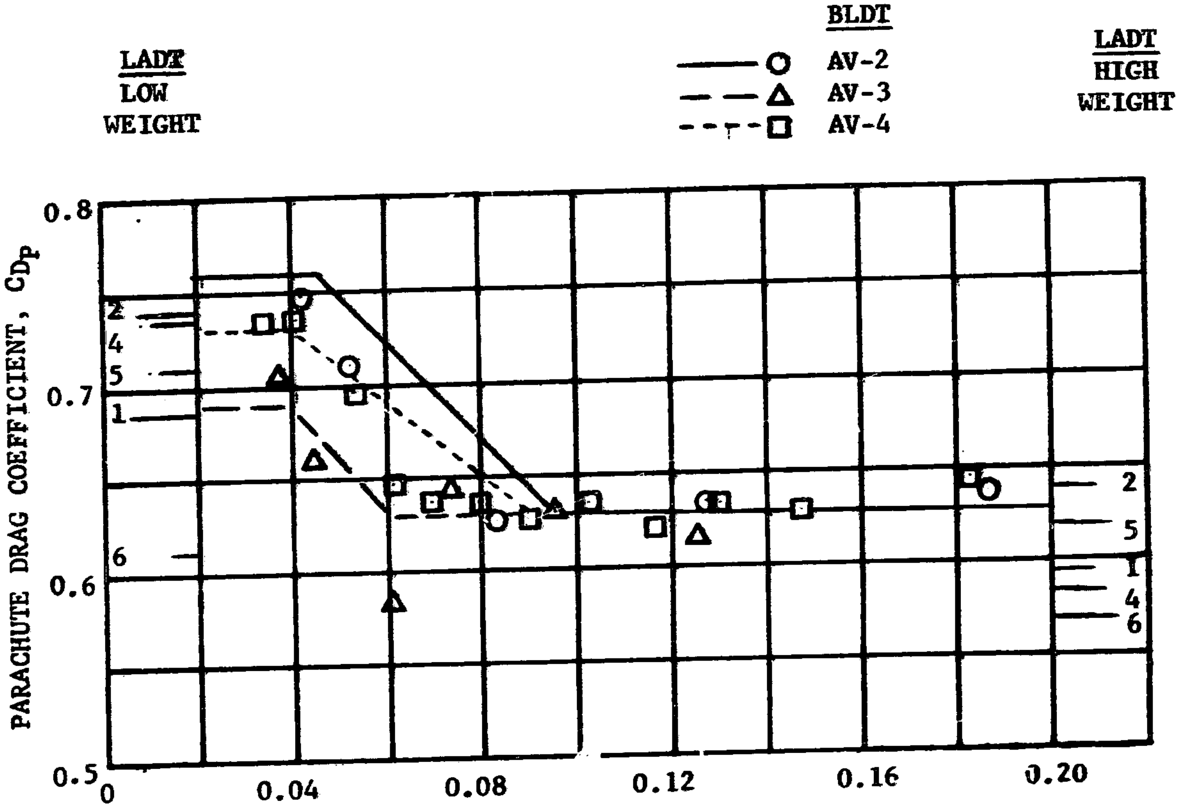

FIGURE 38 COMPARISON BETWEEN LADT AND BLDT DRAG

XIV. CONCLUSIONS

The following major conclusions support the decelerator qualification objectives of the Viking program.

A. The mortar provides sufficient velocity and margin to support full deployment of the parachute.

B. Parachute ejection from mortar fire through line stretch, bag strip and initial inflation is free of significant anomalies.

C. The parachute maintains a very stable drag shape after a short period of initial inflation area oscillations.

D. Sufficient drag performance is produced to support Viking mission requirements and to achieve satisfactory aeroshell separation. The drag coefficient produced by the parachute in the presence of the Viking forebody falls within the required envelope of Figure 28 with few minor deviations of no significance. There is evidence of drag degradation in the wake of the entry vehicle at transonic velocity as was expected.

E. Lander oscillations in quasi-steady state descent with no wind will be less than ±25 degrees on Mars. Attitude rates during terminal descent on Mars will be less than 30 degrees/second. The maximum attitude rate at parachute opening shock will be approximately 100 degrees/second.

F. Parachute structural integrity has been proven supersonically at load conditions approximately 30 percent greater than Mars peak load conditions. Additionally, subsonic development and qualification bomb drop tests have proven the structure at stress levels equivalent to 1.5 times the Mars design values.

The results of the BLDT program and low altitude development and qualification bomb drop tests show that the performance objectives of the Viking decelerator qualification program have been successfully met.

XV. REFERENCES

1. Reichenau, David E. A.: Aerodynamic Characteristics of Disk-Gap-Band Parachutes in the Wake of Viking Entry Forebodies at Mach Numbers from 0.2 to 2.6, AEDC-TR-72-78, July 1972.

2. Hicks, F. et al: Balloon Launched Decelerator Test Program Post-Flight Test Report BLDT Vehicle AV-1. NASA CR 112176, September 1972.

3. Hicks, F. et al: Balloon Launched Decelerator Test Program Post-Flight Test Report BLDT Vehicle AV-2. NASA CR 112177, December 1972.

4. Hicks, F. et al: Balloon Launched Decelerator Test Program Post-Flight Test Report BLDT Vehicle AV-3. NASA CR 112178, January 1973.

5. Hicks, F. et al: Balloon Launched Decelerator Test Program Post-Flight Test Report BLDT Vehicle AV-4. NASA CR 112179, October 1972.

6. Darnell, W.L., Henning, A.B., and Lundstrom, R.R.: Flight Test of a 15-Foot (4.6 Meter) Diameter 120° Conical Spacecraft Simulating Parachute Deployment in a Mars Atmosphere. NASA TN D-4266, 1967.

7. GER-15464: Mortar Development Test Report for Viking Lander Decelerator System, Goodyear Aerospace Corporation, 12 January 1972.

8. GER-15215; Rev. A: Viking Decelerator Design Analysis Report, Goodyear Aerospace Corporation, 20 March 1972.

9. Huckins, E.K.: Techniques for Selection and Analysis of Parachute Deployment Systems, NASA TN D-5619, January 1970.

10. Whitlock, C. H.; Bendura, R. J.: Inflation and Performance of Three Parachute Configurations from Supersonic Flight Tests In a Low-Density Environment, NASA TN D-5296, July 1969.

11. ASD-TR-61-579: Performance and Design Criteria for Deployable Aerodynamic Decelerators, American Power Jet Company, December 1963.

12. Heinrich, H.G. and Noreen, R. A.: Analysis of Parachute Opening Dynamics with Supporting Wind Tunnel Experiments, AIAA Paper 68-924, September 1968.

13. Berndt, R. J. and DeWeese, J. H.: The Opening Force of Solid Cloth, Personnel Type Parachutes, AIAA Paper 70-1167, September 1970.

14. Toni, R.A.: Theory on the Dynamics of a Parachute System Undergoing its Inflation Process, AIAA Paper 70-1170, September 1970.

15. Steinberg, S.: Scale Model Test Results of the Viking Parachute System at Mach Numbers from 0.1 through 2.6, Martin Marietta Corporation, TR-3720181, November 1971.

16. SS-3703004, Viking 75 Project Lander System Specification, Martin Marietta Corporation, November 1972.

17. Moog, R. D.: Viking Vehicle Dynamics Data Book, Martin Marietta Corporation, October 1972.

18. Moog, R. D.: BLDT Data Extrapolation to Mars of Parachute Induced Attitude Rates, Martin Marietta Corporation, Memo 8943-73-11, 17 January 1972.